the motif of the first two cysteines, chemokines are categorized into four major subfamilies: CC, CXC, C, and CX3C chemokines. The most important function of chemokines is their ability to regulate leukocyte recruitment, retention, and trafficking in inflamed tissues (Homey et al., 2002; Ogawa et al., 2004). The expression of several chemokines is increased in the colonic tissue of murine experimental colitis models (Andres et al., 2000; Ajuebor et al., 2004) as well as in colonic biopsy specimens from patients with IBD (Gijsbers et al., 2006). Therefore, much attention has been directed to such chemokines as one of the therapeutic targets for patients with IBD.

CXCL12 was first characterized as pre-B cell growth stimulating factor (Nagasawa et al., 1996a) and is constitutively expressed in stromal cells within the bone marrow (Tokoyoda et al., 2004). Its primary physiologic receptor is CXCR4, which also functions as an entry receptor for strains of human immunodeficiency virus (Bleul et al., 1996). The CXCL12/CXCR4 chemokine axis has an important role in the migration of progenitors during embryonic development of the cardiovascular, hematopoietic, and central nervous systems (Nagasawa et al., 1996b; Tachibana et al., 1998; Zou et al., 1998). Thus, this chemokine axis is considered to serve as a homing beacon during differentiation.

Recent studies showed that this chemokine axis is also involved in several inflammatory diseases, including rheumatoid arthritis (Nanki et al., 2000; Tamamura et al., 2004; Haas et al., 2005), inflammatory liver diseases (Terada et al., 2003; Wald et al., 2004), uveitis (Curnow et al., 2004), and pulmonary fibrosis (Phillips et al., 2004). Nanki et al. (2000) reported that memory T cells highly express CXCR4, and the CXCL12 concentration is extremely high in the synovial fluid of patients with rheumatoid arthritis. Furthermore, Wald et al. (2004) reported that CXCL12 is up-regulated in the endothelium of neoblood vessels of chronically inflamed liver tissues, and $CXCR4^+$ lymphocytes are increased in hepatitis C virus-infected liver tissues with chronic hepatitis. These findings suggest that the CXCL12/CXCR4 axis has an important role in cell trafficking not only in the homeostatic state but also under inflammatory conditions. However, it is not clear whether this chemokine axis is involved in the pathophysiology of IBD.

To elucidate the role of the CXCL12/CXCR4 interaction in colonic inflammation, we first investigated CXCR4 expression on peripheral T cells in patients with IBD. Next, we investigated the expression of both CXCR4 in peripheral T cells and its ligand CXCL12 in the colonic tissue in a dextran sulfate sodium (DSS)-induced colitis mouse model, and then we examined the effect of a CXCR4 antagonist on DSS-induced colitis and interleukin (IL)-10 knockout (KO) mice.

Materials and Methods

Human Samples of Peripheral Blood Cells. Peripheral blood cells were obtained from the following: 17 patients (7 men, 10 women) with active UC; 9 patients (2 men, 7 women) with inactive UC; 8 patients (6 men, 2 women) with active CD; 16 patients (13 men, 3 women) with inactive CD; 6 patients (4 men, 2 women) with infectious colitis; and 5 patients (5 men) as normal controls. Lymphocytes of blood samples were separated by Lymphoprep (Axis-Shield PoC AS, Oslo, Norway). Cells were stained with appropriate fluorochrome-conjugated antibodies (Abs) and were incubated for 30 min at 4°C. Monoclonal antibody against human CD3 (UCHT1) was obtained from eBioscience (San Diego, CA), and anti-human CXCR4 (12G5) and IgG isotype control were obtained from Dako Denmark A/S (Glostrup, Denmark). Stained cells were analyzed with a fluorescence-activated cell sorter (FACS) (Beckman Coulter, Fullerton, CA). To determine disease activity, modified Truelove Witts severity index (MTWSI) was used for patients with UC and CD activity index was used for patients with CD. UC patients who scored >4 on the MTWSI and CD patients who scored >150 on CD activity index were classified to have active disease. Informed consent was obtained from each patient, and the experimental designs of these studies were approved by the Kyoto University Hospital Ethics Committee.

Animals. Female C57BL/6 mice (8–10 weeks of age, weighing 17–20 g) obtained from Japan SLC Inc. (Shizuoka, Japan) and CXCL12/green fluorescent protein (GFP) knockin mice (Tokoyoda et al., 2004) were used for the experiments. They were fed with standard laboratory chow and tap water ad libitum. All mice were housed in specific pathogen-free conditions in the animal facility of Kyoto University. The studies were approved by the animal protection committee of our institution.

Experimental Design of DSS-Induced Colitis. For the induction of colitis, C57BL/6 mice (wild-type and CXCL12/GFP knockin mice) were given 2.5% DSS (molecular mass, 36–50 kDa; MP Biomedicals, Irvine, CA) in their drinking water for 5 days (from day 0 to 4). On day 5, they were switched to regular drinking water. Normal control mice received regular drinking water throughout the experiment.

CXCR4 antagonist TF14016 was obtained from Prof. N. Fuji (Kyoto University, Kyoto, Japan) (Tamamura et al., 2003, 2004). One hundred micrograms of TF14016 dissolved with 200 μl of phosphate-buffered saline (PBS) or 200 μl of PBS alone was administered intraperitoneally once a day during the study period (from day 0 to day 10). Body weight was measured daily throughout the experiment, and mice were killed by cervical dislocation at 10 days after the start of DSS administration. The colonic tissues and mesenteric lymph nodes (MLNs) were removed from each mouse and examined as described below. At necropsy, the length from the ileocecal junction to the anal verge was measured as the colonic length.

Microscopic Assessment of Colonic Damage. The distal third of the colon was evaluated because this segment is most severely affected in DSS-induced colitis (Okayasu et al., 1990). The entire colon was removed, opened longitudinally, and washed with PBS. The distal third of the colon was dissected and then the longitudinal section (1.5 cm from the anal verge) was prepared. For section staining, samples were fixed in acetone and stained with hematoxylin and eosin, and histologically was analyzed in a blind manner. Histological damage was quantified by the histological scoring system described by Williams et al. (2001). In brief, the sections were graded to access inflammation severity, inflammation extent, and crypt damage. The grading index for inflammation severity was as follows: 0, none; 1, mild; 2, moderate; and 3, severe. The grading index for inflammation extent was as follows: 0, none; 1, mucosa; 2, mucosa and submucosa; and 3, transmural. The grading index for crypt damage was as follows: 0, none; 1, basal one-third damaged; 2, basal two-thirds damaged; 3, crypts lost but surface epithelium present; and 4, crypts and surface epithelium lost. Each of these grades was also scored according to the percentage of involvement (0, 0%; 1, 1–25%; 2, 26–50%; 3, 51–75%; and 4, 76–100%). Each subscore (inflammation severity score, inflammation extent score, and crypt damage score) was the product of the grade multiplied by the percentage of involvement. The total colitis score was the sum of the three subscores.

Flow Cytometry Analysis. For analyzing changes of CXCR4 expression on leukocytes, peripheral blood was taken by tail cutting at day 0, 3, 7, and 10 after start of DSS administration. Erythrocytes were removed using lysis buffer (0.16 M NH_4Cl and 0.017 M Tris, adjusted to pH 7.2), and leukocyte population was resuspended in Dulbecco's modified Eagle's medium containing 2% fetal calf serum. Cells (1×10^6) were stained with the appropriate fluorochrome-

conjugated Abs and were incubated for 30 min at 4°C. Monoclonal Abs against granulocyte-differentiation antigen-1 (Gr-1) (RB6-8C5), macrophage adhesion molecule-1 (Mac-1) (M1/70), CXCR4, CD4 (L3T4), CD8 (Ly-2), CD25 (7D4), and rat IgG isotype control were obtained from BD Pharmingen (San Diego, CA). Regulatory T cells ($Foxp3^+$ cells) were stained with the Mouse Regulatory T cell Staining Kit (eBioscience). Stained cells were analyzed with FACSCalibur (BD Biosciences, San Jose, CA). Dead cells were excluded by propidium iodide staining. The data are presented as relative fluorescence intensity or geometric mean fluorescence intensity depicting the degree of the expression of the surface molecule on the cell.

Immunohistochemical Staining and Confocal Microscopy. For section staining, samples were fixed in 4% paraformaldehyde and equilibrated in 30% sucrose/PBS or fixed with acetone for 2 min. Cryostat sections of colonic tissues were stained and mounted with Permafluor (Beckman Coulter). All confocal microscopy was carried out on a LSM 510 META (Carl Zeiss Inc., Thornwood, NY). Monoclonal Abs against α-smooth muscle actin (α-SMA), platelet endothelial cell adhesion molecule-1 (PECAM-1), CD4, CD8, Gr-1, Mac-1 (BD Pharmingen), and mouse IgG (Jackson ImmunoResearch Laboratories Inc., West Grove, PA) were used. For secondary antibodies, Alexa Fluor 546 goat anti-rat or rabbit IgG and Cy5 donkey anti-rat IgG (Jackson ImmunoResearch Laboratories Inc.) were used. Biotinylated antibodies were visualized with streptavidin-Alexa Fluor 546 (Invitrogen, Carlsbad, CA) or streptavidin-Cy5 (Jackson ImmunoResearch Laboratories Inc.).

Isolation and Stimulation of Mesenteric Lymph Node Cells. Mesenteric lymph nodes were collected under sterile conditions in ice-cold medium, and lymph nodes were mechanically disrupted and filtered through a cell strainer (70 μm). Cells (2×10^5/well) were incubated with immobilized anti-CD3 (5 μg/ml, anti-mouse CD3e; BD Pharmingen) in 200 μl of culture medium for 72 h at 37°C in 5% CO_2 air. Cytokine levels in the supernatant of the culture medium were measured by enzyme-linked immunosorbent assay kit (eBioscience).

Quantitative Analysis of RNA Expressions. Samples of colonic tissue for mRNA isolation were removed from the distal third of the colon at 10 days after the start of DSS administration. Total RNA was extracted using the guanidium isothiocyanate-phenol-chloroform method. RNA (1 μg) was reverse transcribed with MultiScribe reverse transcriptase (Applied Biosystems, Foster City, CA), and the resulting complementary DNAs (50 ng/reaction mixture) were analyzed for CXCL12 mRNA expression by real-time polymerase chain reaction using an ABI Prism 7700 sequence detection system (Applied Biosystems). The reaction mixtures were incubated for 2 min at 50°C, denatured for 10 min at 95°C, and subjected to 45 amplification cycles consisting of annealing and extension at 60°C for 1 min followed by denaturation at 95°C for 15 s. The primers and probes used for this experiment were obtained from Applied Biosystems. To quantify isolated RNA and to measure cDNA synthesis efficiency, target cDNAs were normalized to the expression levels of the endogenous reference housekeeping gene, 18S ribosomal RNA (rRNA). The oligonucleotide primers used for CXCL12 rRNA amplification and detection were 5′-CCA GAG CCA ACG TCA AGC AT-3′ (forward) and 5′-CAG CCG TGC AAC AAT CTG AA-3′ (reverse). The oligonucleotide primers used for 18S rRNA amplification and detection were 5′-TAGAGTGTTCAAAGCAGGCCC-3′ (forward) and 5′-CCAACAAATAGAACCGCGGT-3′ (reverse). For simplicity, the expression level of the target gene was expressed as values relative to the control in the experiment.

Migration Assay. Fresh bone marrow cells and MLN cells from C57BL/6 mice were preincubated with or without 1 μM of TF14016 for 30 min at 37°C. Then they were transferred to the upper layer of 3- or 5-μm pore polycarbonate membrane (Transwell; Corning Inc., Corning, NY), which overlaid the lower chamber containing 100 ng/ml CXCL12. After 2 h, a fraction of the cells that migrated to the lower chamber was stained and analyzed by flow cytometry.

Experimental Design of IL-10 KO Mice. Fifty milligrams/mice per day of CXCR4 antagonist, TF14016, or PBS alone was administered intraperitoneally to IL-10 KO mice at 6 weeks of age. Twenty-eight days (4 weeks) after the start of treatment, TF14016 or PBS-treated mice were killed for histological analysis of colonic tissue.

Microscopic Assessment of Chronic Damage in IL-10 KO Mice. Mice were monitored for clinical signs of colitis, including diarrhea and weight loss. At necropsy, samples of the colon (transverse, distal, and proximal) and the rectum were collected and histopathologically examined as described previously. For each section, inflammation (macrophage, lymphocyte, and neutrophil infiltration in the lamina propria or submucosa) was scored for severity according to the following criteria: normal, 0; minimal, 1; mild, 2; moderate, 3; marked, 4; and severe, 5. Gland loss and epithelial hyperplasia were scored by percentage of area involved: none, 0; 1, 1–10% of the mucosa affected; 2, 11–25% affected; 3, 26–50% affected; 4, 51–75% affected; and 5, 76–100% affected. The summed scores for inflammation (lamina propria or submucosa), gland loss, and gland hyperplasia were then determined for each animal. One pathologist without knowledge of this study scored the sections according to standard criteria.

Statistical Analysis. All normalized data were represented as mean ± S.D. In human experiments assessing CXCR4 expression on T cells, the Kruskal-Wallis test with Bonferroni/Dunn analysis was used. A linear regression analysis was used to access the quantitative relation between the intensity of CXCR4 expression on T cells and disease activity. In animal experiments, for two-group comparisons, the Student's unpaired t and Mann-Whitney U tests were used. For multiple comparisons, the Kruskal-Wallis test with Bonferroni/Dunn analysis for nonparametric analysis or two-way analysis of variance with Bonferroni/Dunn ad hoc analyses for parametric analysis was performed. A repeated analysis of variance was performed assess the effect of TF14016 treatment on changes in body weight after an induction of DSS-induced colitis. In experiments using TF14016 treatments, because control mice showed a negligible level of inflammatory cytokine in tissue, one comparison using the unpaired t test was performed. Any significant interaction was detected in multiple comparisons (data not shown). A two-tailed p value of <0.05 was considered statistically significant. The SPSS software package for Windows (version 10; SPSS, Tokyo, Japan) was used.

Results

CXCR4 Expression on Peripheral T Cells Was Increased in Patients with Active UC. First, we examined whether this chemokine axis is involved in human IBD. We investigated CXCR4 expression on peripheral T cells from patients with IBD and with acute infectious colitis compared with those from healthy controls. CXCR4 expression on peripheral T cells in patients with active UC was significantly higher than that in inactive UC and controls, whereas this expression in patients with active CD, inactive CD, inactive UC, and infectious colitis was not different from that in controls (Fig. 1a). Furthermore, there was a significant correlation between CXCR4 expression on peripheral T cells and disease activity (MTWSI) in patients with active UC (Fig. 1b).

Cxcl12 Expression Was Increased in the Colonic Tissue of DSS-Induced Colitis Mice. Next, we investigated the changes of CXCL12 expression in colonic tissue before and after DSS administration using CXCL12/GFP knockin mice. Confocal microscopic analysis was performed before and at 10 days after the start of DSS administration. CXCL12-expressing cells were mainly observed in the perivascular sites of the normal colonic mucosa (Fig. 2, a–d).

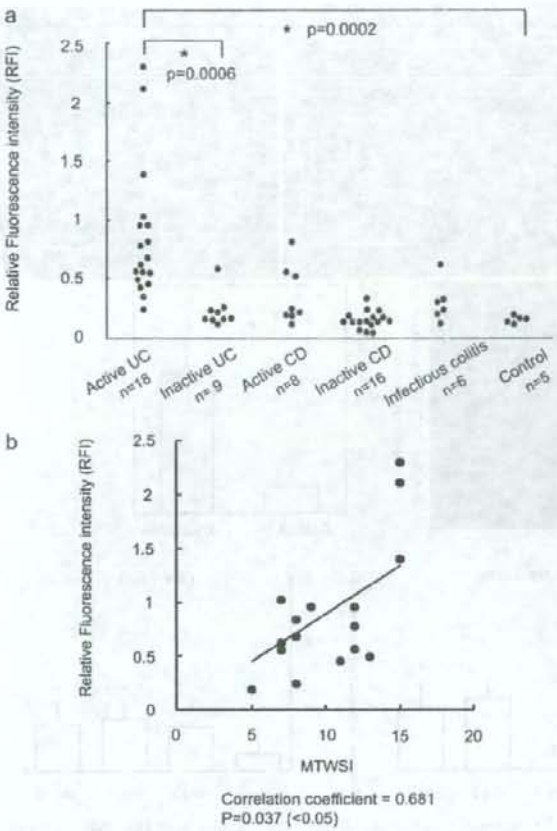

Fig. 1. CXCR4 expressions on peripheral T cells in patients with IBD. a, CXCR4 expression on peripheral T cells from patients with IBD and acute infectious colitis and healthy controls. Eighteen patients with active UC, 9 patients with inactive UC, 8 patients with active CD, 16 patients with inactive CD, 6 patients with infectious colitis, and 5 patients as normal controls. *, $p < 0.05$ compared with inactive UC and normal controls. b, correlation between CXCR4 expression of peripheral T cells and disease activity (MTWSI) in patients with UC.

The CXCL12-expressing cells were morphologically considered to be reticular cells adjacent to the endothelial (PECAM-1$^+$ and/or α-SMA$^+$) cells because they were negative for PECAM-1, α-SMA, and other blood cell marker's staining.

At 10 days after the start of DSS administration, the number of CXCL12-expressing cells was increased in the inflamed colonic mucosa compared with normal colonic tissues (Fig. 2, e and f). Expression of CXCL12 mRNA was also significantly higher in the colonic tissue of mice with DSS-induced colitis (at 10 days after DSS administration) than that of normal mice (Fig. 2g). These results suggest that enhanced CXCL12 expression in the colonic mucosa might induce the migration of inflammatory cells into the inflamed colonic tissues of mice with DSS-induced colitis.

CXCR4 Expression on Peripheral T Cells Is Increased in Mice with DSS-Induced Colitis. To investigate whether the CXCL12/CXCR4 chemotactic axis is involved in DSS-induced colonic inflammation, we analyzed CXCR4 expression on peripheral blood cells from mice with DSS-induced colitis. Serial changes in CXCR4 expression in the peripheral blood cells of these mice were evaluated by flow cytometry. FACS analysis revealed that CXCR4 expression on peripheral granulocytes (Gr-1$^+$ cells) was significantly increased at 7 days and normalized at 10 days after the start of DSS administration. CXCR4 expression on both peripheral CD4$^+$ and CD8$^+$ cells from mice with DSS-induced colitis was also significantly increased at 7 and 10 days (CD4$^+$), and at 3, 7, and 10 days (CD8$^+$) after the start of DSS administration, compared with the levels before DSS administration (day 0) (Fig. 2h).

A CXCR4 Antagonist Efficiently Inhibits Leukocyte Migration to CXCL12 in Vitro. To evaluate whether a CXCR4 antagonist, TF14016, efficiently blocks leukocyte migration toward CXCL12, we performed an in vitro leukocyte chemotaxis assay. Migration analysis showed that the CXCL12-induced chemotactic responses of bone marrow granulocytes and mesenteric CD4$^+$ as well as CD8$^+$ T cells were significantly inhibited by TF14016 (Fig. 3).

Effect of a CXCR4 Antagonist on DSS-Induced Colitis. To investigate whether the blockade of the CXCL12/CXCR4 chemotactic axis attenuates inflammation in DSS-induced colitis, we intraperitoneally administered a CXCR4 antagonist, TF14016, to mice with DSS-induced colitis. During DSS administration, the percentage of body weight in control mice (DSS alone) decreased. The body weight loss of mice with DSS-induced colitis treated with TF14016, however, was significantly lower than that of nontreated mice from 7 to 10 days after the start of DSS administration (Fig. 4a). There was also a significant difference in colonic length between nontreated and TF14016-treated mice with DSS-induced colitis (Fig. 4b).

In mice with DSS-induced colitis, the histologic findings demonstrated epithelial destruction, remarkable inflammatory cell infiltration with lymphoid aggregation, and submucosal edema (Fig. 5a). In contrast, in TF14016-treated mice with DSS-induced colitis, epithelial destruction and inflammatory cell infiltration, including lymphoid aggregation, were obviously reduced compared with nontreated mice (Fig. 5b). As a result, the total colitis score in TF14016-treated mice with DSS-induced colitis was significantly lower than that in the nontreated mice with DSS-induced colitis (Fig. 5c). Immunohistochemical analysis revealed that the number of CD4$^+$ and CD8$^+$ T cells and lymphocyte aggregation in the lamina propria were remarkably decreased in TF14016-treated mice with DSS-induced colitis compared with the nontreated mice with DSS-induced colitis (Fig. 6, a and b).

Blockade of the CXCL12/CXCR4 Axis Reduces the Production of Proinflammatory Cytokines, but Not IL-10 Production, from MLN Cells in Mice with DSS-Induced Colitis. We also measured the cytokine production from unseparated MLN cells from mice with DSS-induced colitis treated with TF14016. The production of tumor necrosis factor (TNF)-α, interferon (IFN)-γ, and IL-10 from unseparated MLN cells was significantly increased in mice with DSS-induced colitis. However, TF14016 treatment significantly reduced the increased production of TNF-α and IFN-γ. In contrast, TF14016 treatment had no effect on the production of IL-10 in mice with DSS-induced colitis (Fig. 7).

Blockade of the CXCL12/CXCR4 Axis Did Not Block the Migration of Foxp3$^+$ Regulatory T Cells to MLN. To elucidate why IL-10 production in MLN cells was not

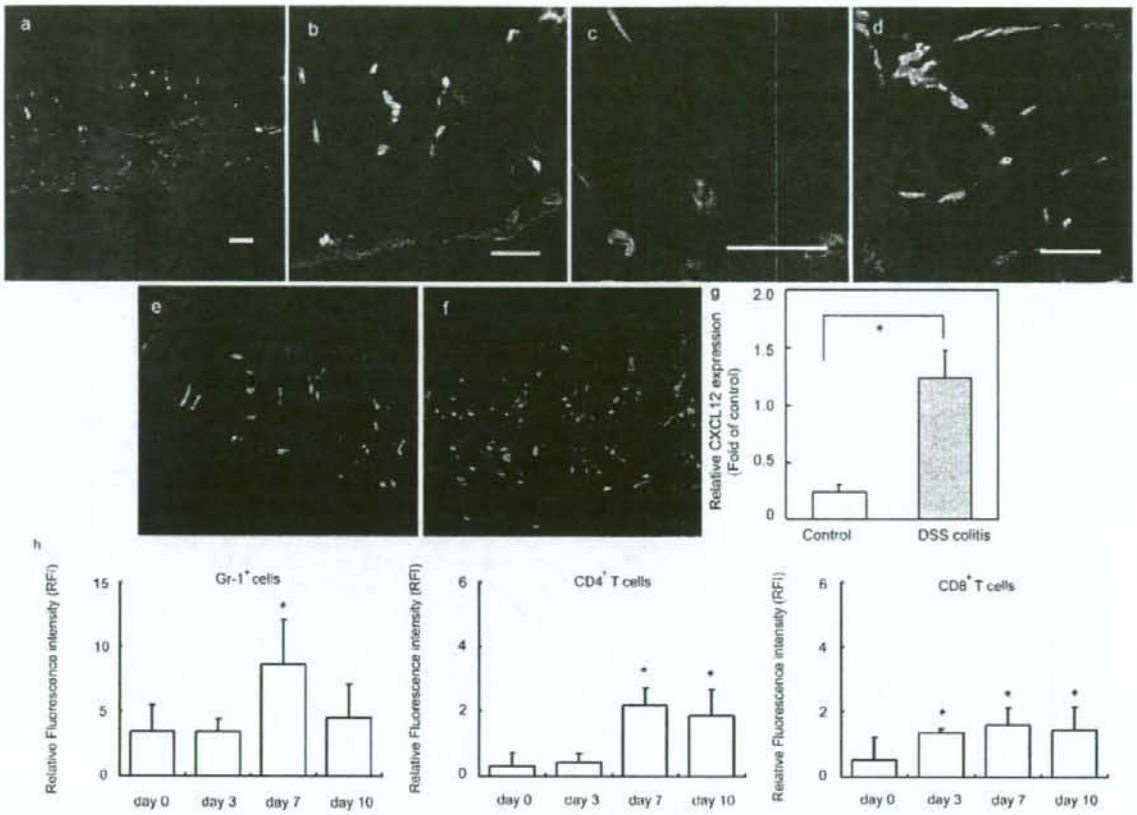

Fig. 2. CXCL12 expression in the colonic tissue and serial changes in CXCR4 expression on peripheral blood cells of mice with DSS-induced colitis. a to d, colonic tissue sections from CXCL12/GFP knockin mice were stained with antibodies against PECAM-1 (blue) and α-SMA (red) (b–d, magnified; b and c, vertical section; d, horizontal section). White bars indicate 20 μm (a) and 10 μm (b–d). e to g, the change of CXCL12 expression was analyzed in CXCL12/GFP knockin mice before (e) and 10 days after the start of DSS administration (f). g, CXCL12mRNA expression in colonic tissues was quantified by quantitative real-time polymerase chain reaction. Results are presented as means ± S.D. ($n = 7$ in each group). *, $p < 0.05$ compared with control mice without DSS. h, Peripheral blood cells were obtained from mice with DSS-induced colitis before and 3, 7, and 10 days after the start of DSS administration. Serial changes of CXCR4 expression on peripheral granulocytes (Gr-1$^+$ cells) and T cells (CD4 and CD8 cells) were evaluated by FACS. Results are presented as means ± S.D. ($n = 5$ in each group). *, $p < 0.05$ compared with normal mice (day 0).

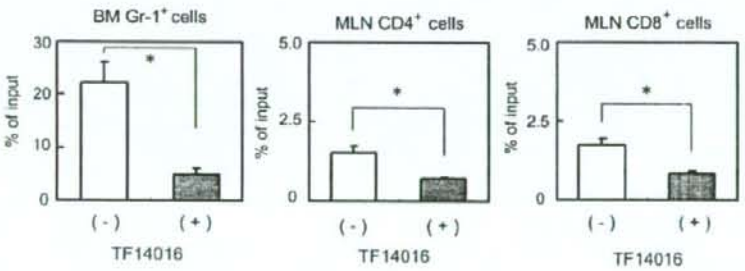

Fig. 3. TF14016 inhibits chemotactic responses to CXCL12 in vitro. CXCL12-induced chemotactic responses of bone marrow granulocytes (Gr-1$^+$ cells) and mesenteric T cells (CD4$^+$ and CD8$^+$ cells) were assessed in the presence (□) or absence (■) of TF14016. Data are expressed as percentage (%) of input of the loaded cells to the lower chamber. Results are presented as means ± S.D. ($n = 4$ in each group). *, $p < 0.05$ compared with leukocytes in the absence of TF14016.

changed by TF14016 treatment despite the decrease in the severity of colitis, we focused on the effect of TF14016 on regulatory T cells, one of MLN's IL-10-producing cells. First, we analyzed CXCR4 expression on regulatory T cells in MLN. In mice with DSS-induced colitis, CXCR4 expression on mesenteric CD4$^+$CD25$^-$ T cells (nonregulatory T cells) was significantly elevated compared with that of normal mice. In contrast, there was no significant difference in CXCR4 expression on mesenteric CD4$^+$CD25$^+$ regulatory T cells between DSS-induced colitis mice and normal mice (Fig. 8a).

We then analyzed the population of Foxp3$^+$ regulatory T cells in MLN. FACS analysis revealed that although the percentage of Foxp3$^+$CD25$^+$ regulatory T cells in MLN was significantly increased in mice with DSS-induced colitis com-

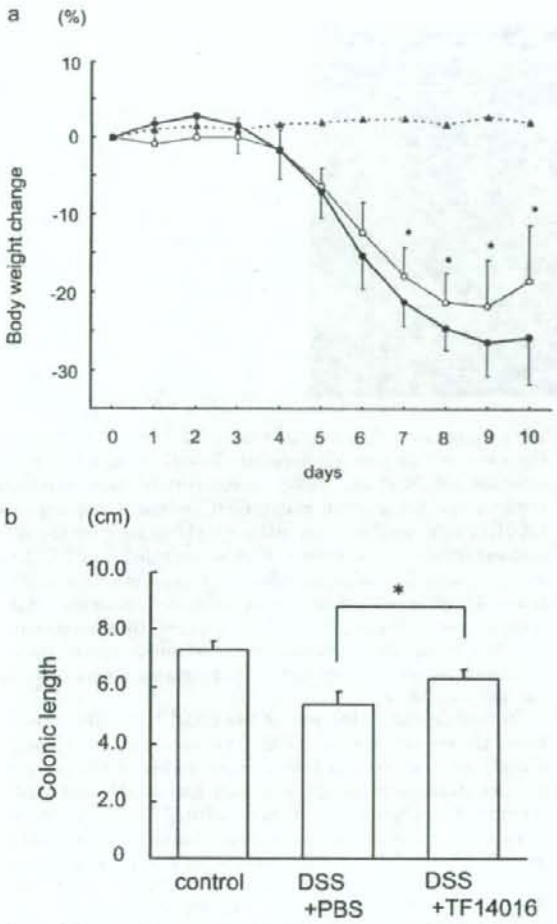

Fig. 4. Therapeutic effect of a CXCR4 antagonist, TF14016, on body weight changes and colonic length in mice with DSS-induced colitis. a, serial changes in body weight were measured daily throughout the experiment. Data are expressed as the mean percentage change from starting body weight. b, colonic length was measured from the ileocecal junction to the anal verge at 10 days after the start of DSS administration. ●, nontreated mice with DSS-induced colitis; ○, mice with DSS-induced colitis treated with TF14016; and ▲, normal mice without DSS. Results are presented as means ± S.D. (n = 10–13 in each group). *, $p < 0.05$ compared with the nontreated mice with DSS-induced colitis.

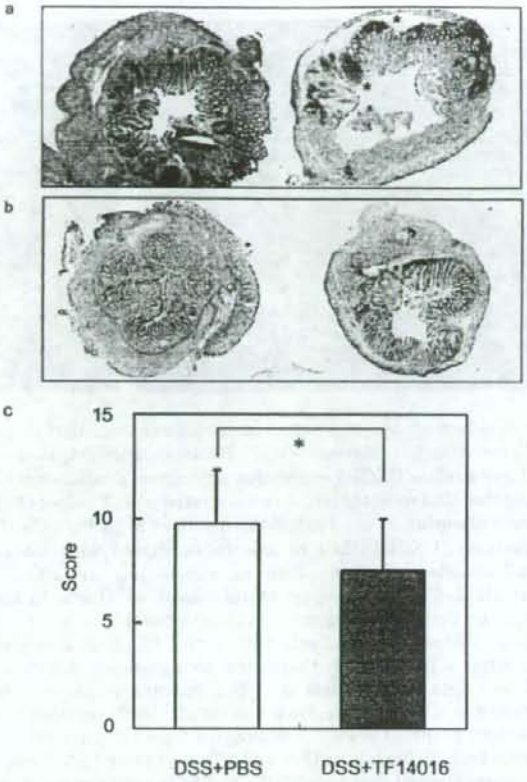

Fig. 5. Histologic changes in colonic tissues of mice with DSS-induced colitis treated with TF14016. a and b, the representative histologic findings of colonic tissues of DSS-induced colitis mice treated with PBS (a) and TF14016 (b) are shown. c, histologic scores of mice with DSS-induced colitis treated with and without TF14016. Results are presented as means ± S.D. (n = 8 in each group). ★, lymphoid aggregation. *, $p < 0.05$ compared with the nontreated mice with DSS-induced colitis.

pared with normal mice, TF14016 treatment did not affect the percentage of $Foxp3^+CD25^+$ regulatory T cells in mice with DSS-induced colitis (Fig. 8b).

Effect of a CXCR4 Antagonist on IL-10 KO Mice. All IL-10 KO mice treated with TF14016 or PBS survived throughout the study period. Histologic examination of colonic tissue from PBS-treated IL-10 KO mice demonstrated epithelial hyperplasia, crypt abscess, and severe acute and chronic cellular infiltration and lymphoid aggregation in lamina propria (Fig. 9a). In contrast, colonic inflammation and amount of lymphocyte aggregation were significantly decreased in IL-10 KO mice treated with a CXCR4 antagonist (Fig. 9b). As shown in Fig. 9c, colonic histological scores in IL-10 KO mice treated with TF14016 were significantly lower than in those treated with PBS alone.

Discussion

The present study demonstrated that CXCR4 expressions on peripheral T cells of active UC patients were significantly higher than those of normal controls, and they were significantly correlated with disease activity. Furthermore, the expression of both CXCR4 on peripheral T cells and CXCL12 in the colonic tissue of mice with DSS-induced colitis were significantly increased compared with normal mice. More importantly, the administration of a CXCR4 antagonist decreased the severity of DSS-induced colitis and colonic inflammation of IL-10 KO mice, as assessed by clinical, histologic, and immunologic parameters. These results strongly suggest that the CXCL12/CXCR4 chemokine axis has an important role in the pathophysiology of IBD, particularly in UC, and that antagonist has a therapeutic effect on experimental colitis.

Previous reports demonstrated that CXCL12 mRNA expression ratio in biopsy specimens from the colonic mucosa of

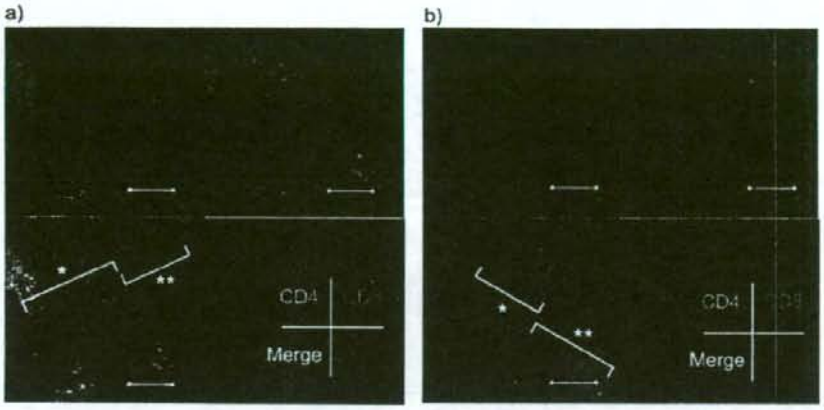

Fig. 6. Confocal microscopic findings of colonic tissues in DSS-induced colitis mice treated with TF14016. The colon sections from mice with DSS-induced colitis treated with PBS (a) or TF14016 (b) were stained with antibody against CD4 (green) and CD8 (red). White bars indicate 100 μm. A representative figure of five mice is shown. *, mucosa-submucosa; **, muscularis propria-serosa.

patients with UC was significantly higher than that in patients with CD (Katsuta et al., 2000). In addition, IL-4 induces surface CXCR4 expression on human T cells, suggesting that this receptor might be associated with T helper (Th)2 cells (Jourdan et al., 1998; Annunziato et al., 1999). On the contrary, CXCR4/CXCL12 axis is associated with several inflammatory diseases such as rheumatoid arthritis, in which IL-6 and TNF-α are mainly involved. Our data also showed that CXCR4 expression in peripheral T cells is likely to be increased in patients with active CD compared with inactive CD, although there was no significant difference. These data may suggest that Th1 immune response is involved in CXCR4 expression. Fuss et al. (1996) reported that lamina propria $CD4^+$ T lymphocytes from UC patients produce both Th1 cytokine IFN-γ and Th2 cytokine IL-5. Several reports showed that anti-TNF-α antibody administration reduced intestinal inflammation in patients with UC (Rutgeerts et al., 2005). Taken together, the immune response in acute flare of UC is very complicated because both Th1 and Th2 immune response and several proinflammatory cytokines are involved. Considering these data, Th2 immune response (IL-4 and IL-5) might augment CXCR4 expression on peripheral T cells under the condition of enhanced Th1 immune response. Accordingly, CXCR4 expression on peripheral T cells was strongly increased in active UC patients and that its expression level was proportional to the disease activity. In this regard, CXCR4 expression on peripheral T cells of patients with UC could be a good marker of their disease activity. However, further investigation will be needed to elucidate the exact mechanism of significant up-regulation of CXCR4 in UC patients compared with CD patients.

In animal models, we investigated CXCL12 expression in colonic tissues using CXCL12/GFP knockin mice because its expression was hardly observed by immunohistochemistry. In the steady state, CXCL12 expression was observed in submucosal lesions, mainly adjacent to the vascular endothelial cells. Based on their location, the majority of CXCL12-expressing cells are considered to be pericytes, mesenchymal-like cells located close to small blood vessel walls. Previous studies (Imai et al., 1999a,b; Peled et al., 1999a; Ponomaryov et al., 2000) reported that human and murine endothelial cell lines express CXCL12 mRNA and produce CXCL12 protein. CXCL12 is expressed on neoblood vessel endothelial cells in the portal tracts and on active lymphoid follicles, suggesting the involvement of CXCL12 in the initial entry of cells into the liver during chronic hepatitis B and hepatitis C virus infection (Wald et al., 2004). In contrast to those previous reports, we found that endothelial cells did not express CXCL12 in colonic tissues, although the reason for the discrepant results is not known. We also revealed that CXCL12 expression in the inflamed colonic tissue of mice with DSS-induced colitis was significantly increased compared with normal mice. These data might suggest that circulating $CXCR4^+$ leukocytes are attracted to inflamed colonic tissues by the increased number of CXCL12-expressing cells at the perivascular sites.

To further clarify the role of the CXCL12/CXCR4 chemokine axis, we next observed CXCR4 expression on peripheral leukocytes in mice with DSS-induced colitis and found that CXCR4 expression on granulocytes and $CD4^+$ and $CD8^+$ lymphocytes is increased in mice with DSS-induced colitis compared with wild-type mice. Thus, it may be reasonable to speculate that those CXCR4-expressing T cells are recruited to the inflamed mucosa of DSS-induced colitis by enhanced expression of CXCL12. The fact that the CXCR4 antagonist ameliorates DSS-induced colitis may further support such possibility. Recent studies have indicated that various cytokines and growth factors, including IL-2, IL-4 (Jourdan et al., 1998), IL-6, stem cell factor (Peled et al., 1999b), vascular endothelial growth factor, basic fibroblastic growth factor, and transforming growth factor-β (Buckley et al., 2000), can enhance CXCR4 expression on a number of cell types. In DSS-induced colitis, the production of various cytokines and growth factors are increased (Dieleman et al., 1994; Matsuura et al., 2005). Accordingly, these cytokines or growth factors might be involved in the induction of CXCR4 expression on granulocytes and T cells in DSS-induced colitis.

CXCR4 expression on T cells was significantly higher at 7 and 10 days after DSS administration than before DSS administration, whereas CXCR4 expression on granulocytes was increased only at day 7. In general, colonic inflammation induced by DSS administration is considered to be mainly caused by direct chemical injury to colonic epithelial cells and activation of resident macrophages and neutrophils (Okayasu et al., 1990; Cooper et al., 1993; Dieleman et al., 1994). However, we found little difference in the infiltration of mononuclear cells or neutrophils in colonic mucosa between mice with DSS-induced colitis and normal mice at 10 days

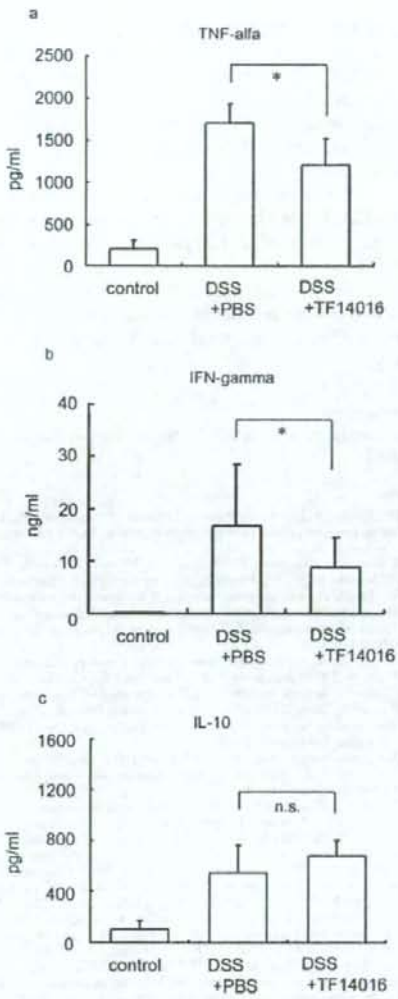

Fig. 7. The cytokine production of MLN cells from DSS-induced colitis mice treated with or without TF14016. MLN cells from mice 10 days after the start of DSS administration were cultured with immobilized anti-CD3. Supernatants were collected after 72 h, and TNF-α (a), IFN-γ (b), and IL-10 (c) were tested by enzyme-linked immunosorbent assay. Results are presented as means ± S.D. ($n = 8$ in each group). *, $p < 0.05$ compared with DSS-induced colitis mice without TF14016 treatment. n.s., not significant.

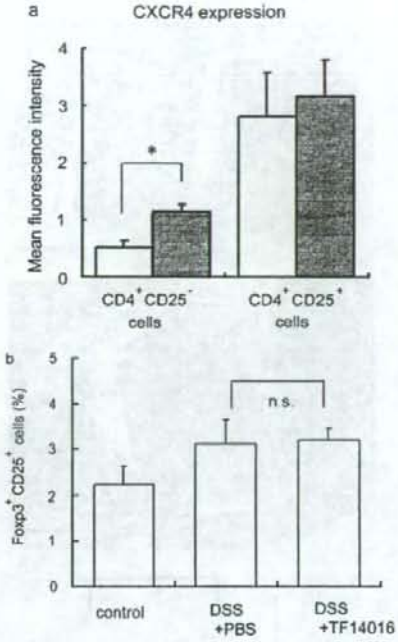

Fig. 8. CXCR4 expression on mesenteric regulatory T cells and the population of mesenteric Foxp3$^+$ regulatory T cells in mice with DSS-induced colitis. a, CXCR4 expression on mesenteric CD4$^+$CD25$^-$ and CD4$^+$CD25$^+$ cells was analyzed before (white bar) and 10 days after starting DSS administration (black bar). b, the population of mesenteric Foxp3$^+$ regulatory T cells from TF14016-treated and the nontreated mice with DSS-induced colitis were analyzed by FACS. Results are presented as means ± S.D. ($n = 5$ in each group). *, $p < 0.05$ compared with normal mice. n.s., not significant.

after starting DSS administration (data not shown). These data suggest that granulocytes are attracted to the inflamed colonic tissue soon after DSS administration by other chemokines like CXCL8/IL-8 and CXCL10/inducible protein-10, the expressions of which are increased during the early phase of DSS-induced colitis (Murano et al., 2000; Melgar et al., 2006). On the other hand, the sustained increase of CXCR4 expression on peripheral T cells at the late phase of DSS-induced colitis, as observed in the present study, suggests that T cells are involved in sustained colonic inflammation after DSS administration in C57BL/6 mice. Melgar et al. (2006) reported that only 5-day administration of DSS induces chronic inflammation of the colon in C57BL/6 mice. Taken together, the increased expression of CXCR4 on T cells might mainly contribute to the development of chronic colitis induced by DSS administration.

An important finding of our study is that blocking the CXCL12/CXCR4 chemotaxis axis significantly ameliorated DSS-induced colitis and colonic inflammation of IL-10 KO mice. Indeed, administration of a CXCR4 antagonist, TF14016, significantly reduced body weight loss of mice with DSS-induced colitis. Moreover, histologic findings revealed that the number of infiltrated lymphocytes and amount of lymphocyte aggregation in both DSS-induced colitis mice and IL-10 KO mice were significantly decreased when treated by the administration of a CXCR4 antagonist. These data strongly support an idea that the CXCL12/CXCR4 chemokine interaction has an important role in the development of experimental colitis, probably through the recruitment of CXCR4-positive lymphocytes to the inflamed colonic mucosa.

It should be noted that although the CXCR4 antagonist significantly reduced the expressions of TNF-α and IFN-γ, it did not alter IL-10 production from MLN cells in mice with DSS-induced colitis, despite the amelioration of colonic inflammation. To clarify the reason for the lack of the effect of the CXCR4 antagonist on IL-10 production, we observed the effect on regulatory T cells in MLN. We first found that although CXCR4 expression on mesenteric CD4$^+$CD25$^-$ cells

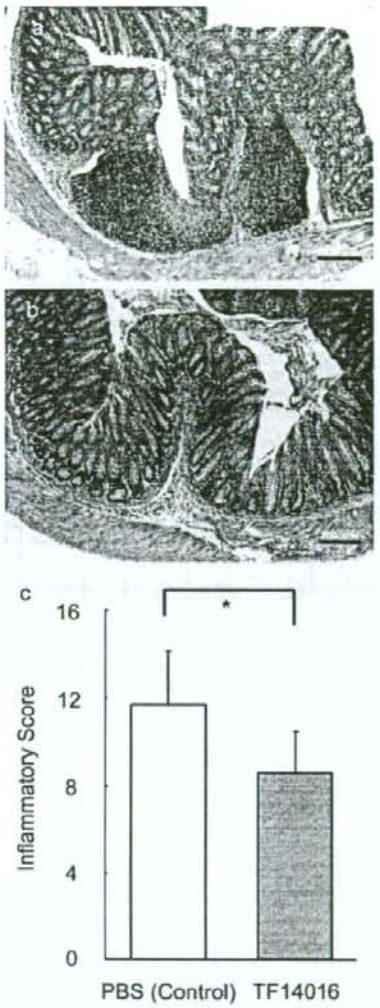

Fig. 9. Administration of a CXCR4 antagonist, TF14016, ameliorated histopathologic features in IL-10 KO mice. a and b, the representative histologic findings of proximal colon sections of IL-10 KO mice treated with PBS (a) and TN14016 (b) are shown. c, histologic scores of IL-10 KO mice treated with and without TF14016. Results are presented as means ± S.D. ($n = 11$ in each group). Black bars indicate 200 μm. *, $p < 0.05$ compared with IL-10 KO mice treated with PBS.

was increased in DSS-induced colitis, there was no significant change in CXCR4 expression on mesenteric $CD4^+CD25^+$ cells. Furthermore, although the percentage of $Foxp3^+CD25^+$ cells in mice with DSS-colitis was significantly higher than normal mice, administration of the CXCR4 antagonist did not affect the percentage of $Foxp3^+CD25^+$ cells. These data indicated that the lack of the effect of CXCR4 antagonist on IL-10 production seems to result from both no increase of CXCR4 expression on regulatory T cells in mice with DSS-induced colitis and no change of the percentage of regulatory T cells by the CXCR4 antagonist administration. Moreover, our data showed that the increased CXCR4 expression on $CD4^+$ T cells in mice with colonic inflammation is mainly attributed to its increased expression on $CD4^+CD25^-$ T cells. Taken together, the present data suggested that the ameliorating action of the CXCR4 antagonist on DSS-induced colitis is mainly due to its inhibitory effect on migration of $CD4^+CD25^-$ T cells with increased CXCR4 expression that seem to be involved in exacerbation of intestinal inflammation in IL-10 KO mice that lack the function of regulatory T cells.

In conclusion, taken together with human and mouse studies, CXCL12/CXCR4 chemokine axis seems to be involved in the pathophysiology of IBD, especially ulcerative colitis. Considering the potent anti-inflammatory effect of the CXCR4 antagonist on experimental colitis, the CXCR4 antagonist might be one of the therapeutic options for patients with IBD. However, further clinical trials will be needed to assess this possibility.

Acknowledgments

We are deeply grateful to Dr. N. Nakao for the statistical support of this article.

References

Ajuebor MN, Kunkel SL, and Hogaboam CM (2004) The role of CCL3/macrophage inflammatory protein-1alpha in experimental colitis. *Eur J Pharmacol* **497**:343–349.

Andres PG, Beck PL, Mizoguchi E, Mizoguchi A, Bhan AK, Dawson T, Koziel WA, Maeda N, MacDermott RP, Podolsky DK, et al. (2000) Mice with a selective deletion of the CC chemokine receptors 5 or 2 are protected from dextran sodium sulfate-mediated colitis: lack of CC chemokine receptor 5 expression results in a $NK1.1^+$ lymphocyte-associated Th2-type immune response in the intestine. *J Immunol* **164**:6303–6312.

Annunziato F, Cosmi L, Galli G, Beltrame C, Romagnani P, Manetti R, Romagnani S, and Maggi E (1999) Assessment of chemokine receptor expression by human Th1 and Th2 cells in vitro and in vivo. *J Leukoc Biol* **65**:691–699.

Bleul CC, Farzan M, Choe H, Parolin C, Clark-Lewis I, Sodroski J, and Springer TA (1996) The lymphocyte chemoattractant SDF-1 is a ligand for LESTR/fusin and blocks HIV-1 entry. *Nature* **382**:829–833.

Blumberg RS, Saubermann LJ, and Strober W (1999) Animal models of mucosal inflammation and their relation to human inflammatory bowel disease. *Curr Opin Immunol* **11**:648–656.

Buckley CD, Amft N, Bradfield PF, Pilling D, Ross E, Arenzana-Seisdedos F, Amara A, Curnow SJ, Lord JM, Scheel-Toellner D, et al. (2000) Persistent induction of the chemokine receptor CXCR4 by TGF-beta 1 on synovial T cells contributes to their accumulation within the rheumatoid synovium. *J Immunol* **165**:3423–3429.

Cooper HS, Murthy SN, Shah RS, and Sedergran DJ (1993) Clinicopathologic study of dextran sulfate sodium experimental murine colitis. *Lab Invest* **69**:238–249.

Curnow SJ, Wloka K, Faint JM, Amft N, Cheung CM, Savant V, Lord J, Akbar AN, Buckley CD, Murray PI, et al. (2004) Topical glucocorticoid therapy directly induces up-regulation of functional CXCR4 on primed T lymphocytes in the aqueous humor of patients with uveitis. *J Immunol* **172**:7154–7161.

Dieleman LA, Ridwan BU, Tennyson GS, Beagley KW, Bucy RP, and Elson CO (1994) Dextran sulfate sodium-induced colitis occurs in severe combined immunodeficient mice. *Gastroenterology* **107**:1643–1652.

Fiocchi C (1998) Inflammatory bowel disease: etiology and pathogenesis. *Gastroenterology* **115**:182–205.

Fuss IJ, Neurath M, Boirivant M, Klein JS, de la Motte C, Strong SA, Fiocchi C, and Strober W (1996) Disparate $CD4^+$ lamina propria (LP) lymphokine secretion profiles in inflammatory bowel disease. Crohn's disease LP cells manifest increased secretion of IFN-gamma, whereas ulcerative colitis LP cells manifest increased secretion of IL-5. *J Immunol* **157**:1261–1270.

Gijsbers K, Gebocs K, and Van Damme J (2006) Chemokines in gastrointestinal disorders. *Curr Drug Targets* **7**:47–64.

Haas CS, Martinez RJ, Attia N, Haines GK 3rd, Campbell PL, and Koch AE (2005) Chemokine receptor expression in rat adjuvant-induced arthritis. *Arthritis Rheum* **52**:3718–3730.

Homey B, Alenius H, Muller A, Soto H, Bowman EP, Yuan W, McEvoy L, Lauerma AI, Assmann T, Bünemann E, et al. (2002) CCL27-CCR10 interactions regulate T cell-mediated skin inflammation. *Nat Med* **8**:157–165.

Imai K, Kobayashi M, Wang J, Ohiro Y, Hamada J, Cho Y, Imamura M, Musashi M, Kondo T, Hosokawa M, et al. (1999a) Selective transendothelial migration of hematopoietic progenitor cells: a role in homing of progenitor cells. *Blood* **93**:149–156.

Imai K, Kobayashi M, Wang J, Shimobu N, Yoshida H, Hamada J, Shindo M, Higashino F, Tanaka J, Asaka M, et al. (1999b) Selective secretion of chemoattractants for hematopoietic progenitor cells by bone marrow endothelial cells: a possible role in homing of hematopoietic progenitor cells to bone marrow. *Br J Haematol* **106**:905–911.

Jourdan P, Abbal C, Noraz N, Hori T, Uchiyama T, Vendrell JP, Bousquet J, Taylor N, Pene J, and Yssel H (1998) IL-4 induces functional cell-surface expression of CXCR4 on human T cells. *J Immunol* **160**:4153–4157.

Katsuta T, Liao C, Shimada K, Shibata K, Mitra P, Banner BF, Mori M, and Barnard

GF (2000) Interleukin-8 and SDF1-alpha mRNA expression in colonic biopsies from patients with inflammatory bowel disease. *Am J Gastroenterol* **95**:3157–3164.
Matsuura M, Okazaki K, Nishio A, Nakase H, Tamaki H, Uchida K, Nishi T, Asada M, Kawasaki K, Fukui T, et al. (2005) Therapeutic effects of rectal administration of basic fibroblast growth factor on experimental murine colitis. *Gastroenterology* **128**:975–986.
Melgar S, Drmotova M, Rehnström E, Jansson L, and Michaëlsson E (2006) Local production of chemokines and prostaglandin E2 in the acute, chronic and recovery phase of murine experimental colitis. *Cytokine* **35**:275–283.
Murano M, Maemura K, Hirata I, Toshina K, Nishikawa T, Hamamoto N, Sasaki S, Saitoh O, and Katsu K (2000) Therapeutic effect of intracolonically administered nuclear factor kappa B (p65) antisense oligonucleotide on mouse dextran sulphate sodium (DSS)-induced colitis. *Clin Exp Immunol* **120**:51–58.
Nagasawa T, Nakajima T, Tachibana K, Iizasa H, Bleul CC, Yoshie O, Matsushima K, Yoshida N, Springer TA, and Kishimoto T (1996a) Molecular cloning and characterization of a murine pre-B-cell growth-stimulating factor/stromal cell-derived factor 1 receptor, a murine homolog of the human immunodeficiency virus 1 entry coreceptor fusin. *Proc Natl Acad Sci U S A* **93**:14726–14729.
Nagasawa T, Hirota S, Tachibana K, Takakura N, Nishikawa S, Kitamura Y, Yoshida N, Kikutani H, and Kishimoto T (1996b) Defects of B-cell lymphopoiesis and bone-marrow myelopoiesis in mice lacking the CXC chemokine PBSF/SDF-1. *Nature* **382**:635–638.
Nanki T, Hayashida K, El-Gabalawy HS, Suson S, Shi K, Girschick HJ, Yavuz S, and Lipsky PE (2000) Stromal cell-derived factor-1-CXC chemokine receptor 4 interactions play a central role in $CD4^+$ T cell accumulation in rheumatoid arthritis synovium. *J Immunol* **165**:6590–6598.
Ogawa H, Iimura M, Eckmann L, and Kagnoff MF (2004) Regulated production of the chemokine CCL28 in human colon epithelium. *Am J Physiol Gastrointest Liver Physiol* **287**:G1062–G1069.
Okayasu I, Hatakeyama S, Yamada M, Ohkusa T, Inagaki Y, and Nakaya R (1990) A novel method in the induction of reliable experimental acute and chronic ulcerative colitis in mice. *Gastroenterology* **98**:694–702.
Peled A, Grabovsky V, Habler L, Sandbank J, Arenzana-Seisdedos F, Petit I, Ben-Hur H, Lapidot T, and Alon R (1999a) The chemokine stimulates integrin-mediated arrest of $CD34^+$ cells on vascular endothelium under shear flow. *J Clin Invest* **104**:1199–1211.
Peled A, Petit I, Kollet O, Magid M, Ponomaryov T, Byk T, Nagler A, Ben-Hur H, Many A, Shultz L, et al. (1999b) Dependence of human stem cell engraftment and repopulation of NOD/SCID mice on CXCR4. *Science* **283**:845–848.
Phillips RJ, Burdick MD, Hong K, Lutz MA, Murray LA, Xue YY, Belperio JA, Keane MP, and Strieter RM (2004) Circulating fibrocytes traffic to the lungs in response to CXCL12 and mediate fibrosis. *J Clin Invest* **114**:438–446.
Ponomaryov T, Peled A, Petit I, Taichman RS, Habler L, Sandbank J, Arenzana-Seisdedos F, Magerus A, Caruz A, Fujii N, et al. (2000) Induction of the chemokine stromal-derived factor-1 following DNA damage improves human stem cell function. *J Clin Invest* **106**:1331–1339.
Rutgeerts P, Sandborn WJ, Feagan BG, Reinisch W, Olson A, Johanns J, Travers S, Rachmilewitz D, Hanauer SB, Lichtenstein GR, et al. (2005) Infliximab for induction and maintenance therapy for ulcerative colitis. *N Engl J Med* **8**:2462–2476.
Sartor RB (1995) Current concepts of the etiology and pathogenesis of ulcerative colitis and Crohn's disease. *Gastroenterol Clin North Am* **24**:475–507.
Tachibana K, Hirota S, Iizasa H, Yoshida H, Kawabata K, Kataoka Y, Kitamura Y, Matsushima K, Yoshida N, Nishikawa S, et al. (1998) The chemokine receptor CXCR4 is essential for vascularization of the gastrointestinal tract. *Nature* **393**:591–594.
Tamamura H, Hiramatsu K, Mizumoto M, Ueda S, Kusano S, Terakubo S, Akamatsu M, Yamamoto N, Trent JO, Wang Z, et al. (2003) Enhancement of the T140-based pharmacophores leads to the development of more potent and bio-stable CXCR4 antagonists. *Org Biomol Chem* **1**:3663–3669.
Tamamura H, Fujisawa M, Hiramatsu K, Mizumoto M, Nakashima H, Yamamoto N, Otaka A, and Fujii N (2004) Identification of a CXCR4 antagonist, a T140 analog, as an anti-rheumatoid arthritis agent. *FEBS Lett* **569**:99–104.
Terada R, Yamamoto K, Hakoda T, Shimada N, Okano N, Baba N, Ninomiya Y, Gershwin ME, and Shirateri Y (2003) Stromal cell-derived factor-1 from biliary epithelial cells recruits CXCR4-positive cells: implications for inflammatory liver diseases. *Lab Invest* **83**:665–672.
Takoyoda K, Egawa T, Sugiyama T, Choi BI, and Nagasawa T (2004) Cellular niches controlling B lymphocyte behavior within bone marrow during development. *Immunity* **20**:707–718.
Wald O, Pappo O, Safdi R, Dagan-Berger M, Beider K, Wald H, Franitza S, Weiss I, Avniel S, Bosz P, et al. (2004) Involvement of the CXCL12/CXCR4 pathway in the advanced liver disease that is associated with hepatitis C virus or hepatitis B virus. *Eur J Immunol* **34**:1164–1174.
Williams KL, Fuller CR, Dieleman LA, DaCosta CM, Haldeman KM, Sartor RB, and Lund PK (2001) Enhanced survival and mucosal repair after dextran sodium sulfate-induced colitis in transgenic mice that overexpress growth hormone. *Gastroenterology* **120**:925–937.
Zou YR, Kottmann AH, Kuroda M, Taniuchi I, and Littman DR (1998) Function of the chemokine receptor CXCR4 in haematopoiesis and in cerebellar development. *Nature* **393**:595–599.

Address correspondence to: Dr. Hiroshi Nakase, Department of Gastroenterology and Hepatology, Graduate School of Medicine, Kyoto University, 54 Shogoin Kawahara-Cho, Sakyoku, Kyoto 606-8507, Japan. E-mail: hiropy_n@kuhp.kyoto-u.ac.jp

doi:10.1038/nature07240

LETTERS

ATP drives lamina propria T_H17 cell differentiation

Koji Atarashi[1]*, Junichi Nishimura[1]*, Tatsuichiro Shima[2], Yoshinori Umesaki[2], Masahiro Yamamoto[1,3], Masaharu Onoue[2], Hideo Yagita[4], Naoto Ishii[5], Richard Evans[6], Kenya Honda[1,3] & Kiyoshi Takeda[1,3]

Interleukin (IL)-17-producing CD4$^+$ T lymphocytes (T_H17 cells) constitute a subset of T-helper cells involved in host defence and several immune disorders[1,2]. An intriguing feature of T_H17 cells is their selective and constitutive presence in the intestinal lamina propria[3]. Here we show that adenosine 5′-triphosphate (ATP) that can be derived from commensal bacteria activates a unique subset of lamina propria cells, CD70^{high}CD11c^{low} cells, leading to the differentiation of T_H17 cells. Germ-free mice exhibit much lower concentrations of luminal ATP, accompanied by fewer lamina propria T_H17 cells, compared to specific-pathogen-free mice. Systemic or rectal administration of ATP into these germ-free mice results in a marked increase in the number of lamina propria T_H17 cells. A CD70^{high}CD11c^{low} subset of the lamina propria cells expresses T_H17-prone molecules, such as IL-6, IL-23p19 and transforming-growth-factor-β-activating integrin-αV and -β8, in response to ATP stimulation, and preferentially induces T_H17 differentiation of co-cultured naive CD4$^+$ T cells. The critical role of ATP is further underscored by the observation that administration of ATP exacerbates a T-cell-mediated colitis model with enhanced T_H17 differentiation. These observations highlight the importance of commensal bacteria and ATP for T_H17 differentiation in health and disease, and offer an explanation of why T_H17 cells specifically present in the intestinal lamina propria.

The intestinal mucosa has a unique and complicated immune system composed of a variety of cell populations. Among these, T_H17 cells, a subset of CD4$^+$ T cells characterized by their STAT3-dependent expression of RORγt (encoded by *Rorc*) and production of IL-17, IL-22 and IL-21, control a variety of bacterial and fungal infections at mucosal surfaces[1–7]. Importantly, aberrant T_H17 responses have been implicated in the pathogenesis of inflammatory bowel diseases[8]. The development of T_H17 cells has been shown to be controlled by the local cytokine milieu, including IL-6, transforming growth factor-β (TGF-β) and IL-23 (refs 1, 2, 7, 9–12). However, the mechanism of T_H17 development in the intestine is as yet not fully understood.

IL-17-expressing cells constitute a considerable proportion of CD4$^+$ cells in the intestinal lamina propria, even in healthy mice kept under specific-pathogen-free (SPF) conditions (Supplementary Fig. 1a and ref. 3). The colonic lamina propria CD4$^+$ cells also express messenger RNAs for IL-17, IL-17F and RORγt, representing the hallmarks of T_H17 cells (Supplementary Fig. 1b). The number of these 'naturally occurring' T_H17 cells in the colonic lamina propria increases with age (Supplementary Fig. 1c). Although interferon (IFN)-γ-positive CD4$^+$ cells are similarly observed in the lamina propria and spleen, IL-17-producing cells are rarely observed in the spleen, mesenteric lymph node (MLN) or Peyer's patches (Supplementary Fig. 1a and ref. 3). Furthermore, the lamina propria IL-17-producing CD4$^+$ cells were normally observed in Peyer's-patch- and colonic-patch-null mice[13] (Supplementary Fig. 2). These observations suggest that a specific environment in the lamina propria supports the generation of T_H17 cells *in situ*.

To investigate whether intestinal commensal bacteria are responsible for the generation of lamina propria T_H17 cells, we evaluated the numbers of T_H17 cells in germ-free mice. Although the numbers of colonic lamina propria CD4$^+$ cells were not significantly changed (Supplementary Fig. 3a), the numbers of IL-17-positive CD4$^+$ cells were greatly reduced in the large intestines of germ-free mice compared to those in SPF mice (Fig. 1a, b and Supplementary Fig. 3b). Consistent with previous reports[14], the germ-free mice also exhibited severe reductions in their faecal IgA levels (Supplementary Fig. 3c), demonstrating that commensal bacteria contribute to the provision of a particular environment for lamina propria T_H17 cells as well as IgA-producing cells. To examine the role of commensal bacteria further, we treated SPF mice with a combination of vancomycin and metronidazole by oral administration, and analysed lamina propria T_H17 cells. The vancomycin- and metronidazole-treated mice showed marked reductions in both their faecal IgA levels and their numbers of IL-17-producing CD4$^+$ cells (Supplementary Fig. 4a–c).

To assess the molecular basis for the commensal-bacteria-driven T_H17 differentiation, we examined the contribution of Toll-like receptor (TLR) signalling using *Myd88*$^{-/-}$*Trif*$^{-/-}$ mice, which lack all TLR signalling. There was no detectable difference in the numbers of lamina propria IL-17-producing CD4$^+$ cells between control and mutant animals (Fig. 1c, d and Supplementary Fig. 3d), indicating that the development of lamina propria T_H17 cells is independent of TLR signalling. It is worth noting that *Myd88*$^{-/-}$*Trif*$^{-/-}$ mice showed impaired secretion of IgA in their faecal pellets (Supplementary Fig. 3e), indicating that the development of intestinal T_H17 cells and IgA-producing cells are both dependent on microflora, but are regulated by different mechanisms.

ATP has recently been shown to modulate immune cell functions by means of activation of the ATP sensors, P2X and P2Y receptors[15–18]. In addition, bacteria have been shown to generate and secrete large amounts of ATP[19]. Indeed, ATP concentrations in faecal samples without bacterial lysis were much higher in SPF mice than in germ-free mice (Fig. 1e). Consistent with this result, ATP concentrations were reduced in faecal samples from SPF mice treated with vancomycin and metronidazole (Supplementary Fig. 4d). Furthermore, high ATP concentration was detected in the supernatant of *in vitro* cultured intestinal commensal bacteria derived from faeces of SPF mice (Supplementary Fig. 5). Therefore, although there might be other cellular sources of ATP such as dead epithelial cells, commensal bacteria may be a major source of intestinal luminal ATP. Interestingly, the faecal ATP concentrations were not reduced in

[1]Laboratory of Immune Regulation, Graduate School of Medicine, Osaka University, 2-2 Yamadaoka, Suita, Osaka 565-0871, Japan. [2]Yakult Central Institute for Microbiological Research, Yaho 1796, Kunitachi, Tokyo 186-8650, Japan. [3]WPI Immunology Frontier Research Center, Osaka University, Osaka 565-0871, Japan. [4]Department of Immunology, Juntendo University School of Medicine, 2-1-1 Hongo, Bunkyo-ku, Tokyo 113-8421, Japan. [5]Department of Microbiology and Immunology, Tohoku University Graduate School of Medicine, 2-1 Seiryo-machi, Aoba-ku, Sendai 980-8575, Japan. [6]Department of Cell Physiology and Pharmacology, Henry Wellcome Building 2/59b, University of Leicester, Leicester LE1 9HN, UK.
*These authors contributed equally to this work.

Myd88$^{-/-}$*Trif*$^{-/-}$ mice (Fig. 1f). These results prompted us to examine the contribution of ATP to the generation of intestinal T_H17 cells. To this end, we treated germ-free mice with a non-hydrolysable ATP analogue, ATPγS (ref. 15), by intraperitoneal or rectal administration, and analysed the numbers of lamina propria IL-17-producing cells. The numbers of IL-17-producing CD4$^+$ cells were markedly increased in the ATPγS-treated germ-free mice (Fig. 1g–i). In contrast, ATP injection affected neither the numbers of IFN-γ-producing CD4$^+$ cells (Fig. 1g, h) nor faecal IgA levels (Supplementary Fig. 3f). To assess further the possible involvement of ATP in T_H17 differentiation, we treated SPF mice with an ATP-hydrolysing enzyme, apyrase, or with an antagonist of P2X receptors, 2′,3′-*O*-(2,4,6-trinitrophenyl)-ATP (TNP-ATP)[15]. In the apyrase- or TNP-ATP-treated mice, the numbers of IL-17-producing lamina propria CD4$^+$ cells were significantly reduced (Fig. 1j, k), suggesting the key role of ATP in the generation of intestinal T_H17 cells.

Accumulating evidence suggests that lamina propria CD11c$^+$ antigen-presenting cells directly sample the luminal contents and activate T cells[20,21]. Indeed, the induction of mRNAs for IL-6 (encoded by *Il6*), IL-23p19 (*Il23a*) and integrin-αV (*Itgav*) and -β8 (Itgb8) was observed in lamina propria CD11c$^+$ cells, but not in CD11c$^-$ cells or epithelial cells, harvested from ATPγS-treated germ-free mice (Supplementary Fig. 6). Integrin-αV and -β8 are known to be involved in the activation of latent complexes of TGF-β[22]. Therefore, we assumed that ATP promotes T_H17 differentiation by means of stimulation of lamina propria CD11c$^+$ cells. Accordingly, we next co-cultured lamina propria CD11c$^+$ cells with splenic naive CD4$^+$CD62L$^+$ T cells in the presence of a culture supernatant of intestinal commensal bacteria, which contained a high amount of ATP (Supplementary Fig. 5). Addition of this supernatant markedly enhanced differentiation of IL-17-expressing cells, but not of IFN-γ-expressing cells (Fig. 2a). This T_H17 differentiation was severely inhibited by the presence of apyrase. In contrast, a culture supernatant from *Salmonella typhimurium* showed a lower concentration of ATP and weaker ability to induce T_H17 differentiation (Fig. 2a and Supplementary Fig. 5). Notably, the culture supernatant from *S. typhimurium* potently induced T_H1 differentiation, but this was not inhibited by apyrase (Fig. 2a).

To assess whether ATP was sufficient to induce T_H17 differentiation, we co-cultured lamina propria or splenic CD11c$^+$ cells with splenic naive CD4$^+$ cells in the presence of ATPγS. The expression levels of *Il17a*, *Il17F*, *Il21* and *Il22*, but not *Ifng*, were markedly increased in CD4$^+$ cells cultured with lamina propria CD11c$^+$ cells in the presence of ATPγS (Fig. 2b and Supplementary Fig. 7a). The T_H17 differentiation was also enhanced by another non-hydrolysable form of ATP, α,β-methylene-ATP (αβ-ATP), and weakly enhanced by 2,3-*O*-(4-benzoylbenzoyl)-ATP (Bz-ATP)[15] (Supplementary Fig. 7b). *Myd88*$^{-/-}$*Trif*$^{-/-}$ CD11c$^+$ cells and control cells exerted a similar effect on CD4$^+$ cells, ruling out the possibility of endotoxin contamination (Supplementary Fig. 7c). The effect by ATPγS or αβ-ATP on T_H17 differentiation was inhibited by pharmacological blockade of P2X and P2Y receptors using suramin, or a combination of TNP-ATP and brilliant blue G[15] (Supplementary Fig. 8). Importantly, these inhibitors had no effect

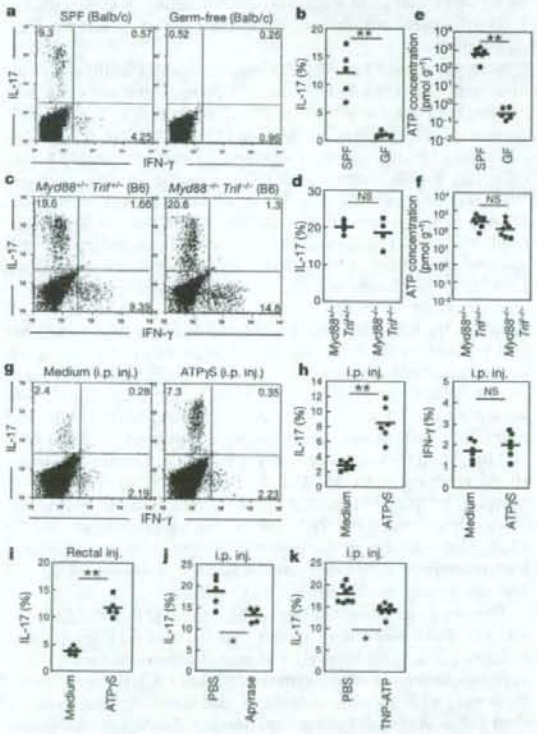

Figure 1 | Administration of ATP leads to a marked increase in lamina propria T_H17 cells in otherwise T_H17-lacking germ-free mice. **a**–**d**, Representative FACS dot plots gated on colonic lamina propria CD4$^+$ cells in the indicated mice are shown in **a** and **c**, and the percentages of IL-17-producing CD4$^+$ cells of individual mice are shown in **b** and **d**. GF, germ free. **e**, **f**, Faecal ATP levels (pmol per g faeces) in the indicated individual mice. **g**–**k**, Germ-free mice (ICR) were daily injected intraperitoneally (i.p.) or rectally with medium or ATPγS (**g**–**i**). SPF mice were i.p. injected with PBS or apyrase, or with TNP-ATP (**j**, **k**). All mice were processed for FACS as in **a**–**d**. All experiments were performed more than twice with similar results. Horizontal bars indicate the means. $^{**}P < 0.01$, $^{*}P < 0.05$; NS, not significant.

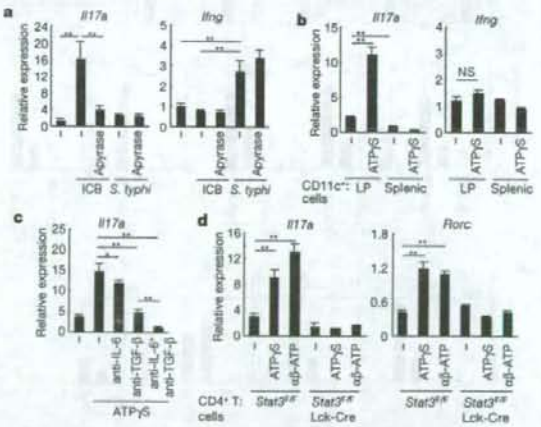

Figure 2 | ATP induces differentiation of naive CD4$^+$ T cells into T_H17 cells. **a**, Splenic naive CD4$^+$ T cells were co-cultured with colonic lamina propria CD11c$^+$ with 20% conditioned medium from cultures of intestinal commensal bacteria (ICB) or *S. typhimurium* (*S. typhi*) in the presence or absence of apyrase. After 4 days, T cells were collected, restimulated and assayed for expression of *Il17* and *Ifng* by rRT–PCR. **b**, **c**, rRT–PCR analyses for the indicated genes of splenic naive CD4$^+$ T cells cultured with colonic lamina propria (LP) or splenic CD11c$^+$ cells in the presence of ATPγS (**b**) with or without anti-IL-6, anti-TGF-β or their combination (**c**). **d**, rRT–PCR analyses for the indicated genes of splenic naive CD4$^+$ T cells from *Stat3*$^{F/F}$ Lck-Cre or *Stat3*$^{F/F}$ mice cultured with wild-type colonic LP CD11c$^+$ cells in the presence of ATPγS or αβ-ATP. Error bars, s.d. $^{*}P < 0.05$, $^{**}P < 0.01$. Representative results are shown from one of two to five independent experiments.

on, or slightly enhanced, T_H1 cell differentiation. Although there might be other molecules affected by the ATP analogues and inhibitors we used, our results support the notion that the specific effect of ATP on T_H17 differentiation was mediated by P2X and P2Y receptors. The ATP-mediated enhancement of T_H17 differentiation was inhibited by anti-IL-6 or anti-TGF-β antibodies, and more severely inhibited by the combination of both antibodies (Fig. 2c). Consistent with this result, *Il6*$^{-/-}$ CD11c$^+$ cells failed to induce the differentiation of IL-17-producing cells in response to ATP (Supplementary Fig. 7d). In addition, no effects of ATP on the differentiation of cells expressing *Il17a* and *Rorc* were observed for CD4$^+$ cells from *Stat3*$^{F/F}$ mice crossed onto Lck-Cre mice (*Stat3*$^{F/F}$ Lck-Cre mice), in which the *Cre* transgene is under the control of the *Lck* promoter[23] (Fig. 2d). These results suggest that ATP stimulates lamina propria CD11c$^+$ cells to produce IL-6 and TGF-β, thereby promoting the T_H17 differentiation by activation of STAT3 in CD4$^+$ cells.

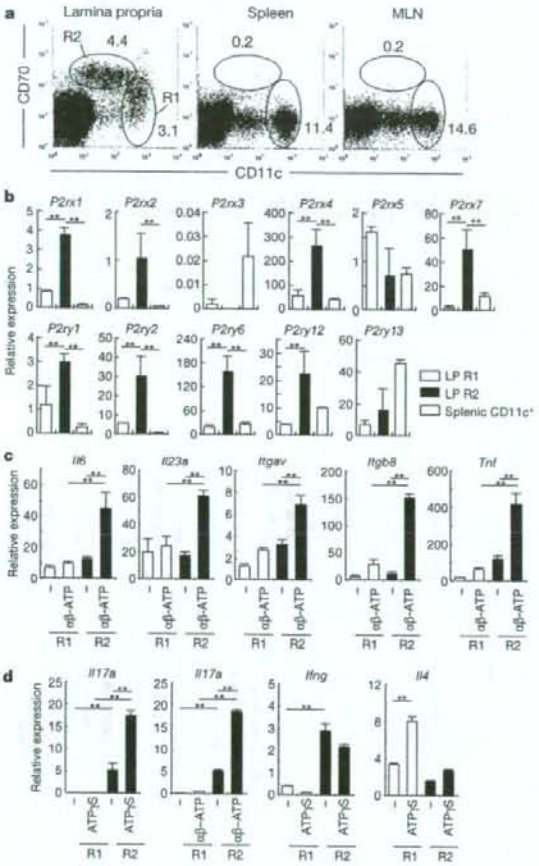

Figure 3 | A unique subset of lamina propria CD11c$^+$ cells express P2X and P2Y receptors. a, Flow cytometry of cells isolated from the colonic lamina propria, spleen or MLN. Numbers indicate the percentages of CD70^{low}CD11c^{high} cells (R1) or CD70^{high}CD11c^{low} cells (R2). **b**, rRT–PCR analyses for P2X and P2Y receptors in R1, R2 or splenic CD11c$^+$ cells. **c**, The sorted R1 and R2 cells were stimulated with αβ-ATP for 3 h and assayed for expression of the indicated genes. **d**, The sorted R1 and R2 cells were co-cultured with splenic naive CD4$^+$ T cells with ATPγS or αβ-ATP for 4 days. The levels of indicated mRNAs in the co-cultured T cells were analysed by rRT–PCR. Data are presented as means + s.d. of triplicate determinations. All experiments were performed more than three times with similar results. $^{**}P < 0.01$.

The heterogeneity of lamina propria CD11c$^+$ cells has been addressed in a number of studies[24]. Therefore, we investigated which subsets of lamina propria CD11c$^+$ cells mediate T_H17 development. Flow cytometry analyses led to the identification of two major CD11c$^+$ populations in the colonic lamina propria: CD70^{low}CD11c^{high} cells (termed R1) and CD70^{high}CD11c^{low} cells (termed R2; Fig. 3a). The R2 population comprised a unique subset present in the lamina propria (Fig. 3a). This subset was positive for myeloid lineage cell markers, such as F4/80 and CD11b, and exhibited immune-activating properties, as was evident from their high expression of CD70 and CD80, but was negative for the immune-suppressive marker CD103 (Supplementary Fig. 9a and refs 25 and 26). R2 cells also expressed CX3CR1; thus, this population seems to be a part of the previously described CX3CR1$^+$CD11b^{high}CD11c^{low} T_H17-inducing subset[16] (Supplementary Fig. 9a–c). R2 cells were observed in the lamina propria of germ-free mice or Peyer's-patch- and colonic-patch-null mice (Supplementary Fig. 11a, b), suggesting that this subset of cells develop by means of microflora- and Peyer's-patch-/colonic-patch-independent mechanisms. Because treatment with a blocking antibody for CD70 or deficiency of CD27, a receptor for CD70 (ref. 27), did not influence the number of lamina propria T_H17 cells (data not shown), CD70 itself is dispensable for T_H17 differentiation.

Next, we sorted R1 or R2 cells (Supplementary Fig. 10) and examined their expression of P2X and P2Y receptors by real-time polymerase chain reaction with reverse transcription (rRT–PCR). R2 cells expressed higher levels of mRNA for P2X1, P2X2, P2X4, P2X7, P2Y1, P2Y2, P2Y6 and P2Y12 receptors than R1 cells or splenic CD11c$^+$ cells (Fig. 3b). Furthermore, R2 cells expressed *Il6*, *Il23a Itgav* and *Itgb8* in response to ATP (Fig. 3c). In addition, on ATP stimulation, R2 cells expressed tumour necrosis factor-α (TNF-α), which has been implicated in T_H17 responses in humans[28]. R2 cells, but not R1 cells, efficiently induced the differentiation of co-cultured naive CD4$^+$CD62L$^+$ T cells into IL-17-expressing cells, and this effect was markedly enhanced by the presence of ATP (Fig. 3d). Although the R2 population also induced T cells to differentiate into IFN-γ-positive cells, this effect was not enhanced by ATPγS (Fig. 3d). In this experimental setting, IL-4-expressing cells were also induced, but this effect was more remarkable in co-cultures with R1 cells, suggesting that R1 and R2 cells carry out distinct missions with each other. R2 cells present in germ-free mice expressed low levels of *Il6* and *Itgb8*, and showed lower ability to induce T_H17 differentiation of co-cultured naive CD4$^+$ T cells (Supplementary Fig. 11c, d); however, by the addition of ATPγS, R2 cells from germ-free mice efficiently enhanced the T_H17 differentiation (Supplementary Fig. 11d). These results all support the hypothesis that commensal-bacteria-derived ATP is responsible for the activation of R2 cells and subsequent development of T_H17 cells.

To extend our understanding of the role of ATP in the differentiation of T_H17 cells, we examined the effects of ATP on intestinal inflammation. We adoptively transferred naive wild-type CD4$^+$ T cells into severe combined immunodeficient (SCID) mice[29], treated these mice with αβ-ATP or medium, and monitored the severity of their colitis. Although both groups developed colitis, treatment with αβ-ATP exacerbated the symptoms of the disease, including diarrhoea and weight loss (Fig. 4a, Supplementary Fig. 12a and data not shown). Extensive oedema was prominent in the colon of αβ-ATP-treated SCID mice (Supplementary Fig. 12b). Histological analyses revealed that inflammatory cell infiltration, epithelial hyperplasia and loss of goblet cells were more evident in the colon of αβ-ATP-treated SCID mice (Fig. 4b). Notably, in contrast to a lack of considerable effect on IFN-γ-positive cells, the number of IL-17-positive CD4$^+$ cells was significantly increased in the αβ-ATP-treated SCID mice (Fig. 4c, d and Supplementary Fig. 12c). Thus, ATP-induced deterioration of colitis was accompanied by an increase in the

number of T_H17 cells in this T-cell-mediated colitis model, indicating the possible involvement of ATP in the generation of 'pathogenic' T_H17 cells.

From our results, we propose the following scenario: commensal-bacteria-derived ATP activates $CD70^{high}CD11c^{low}$ cells in the lamina propria to induce IL-6 and IL-23 production as well as TGF-β activation, thereby leading to local differentiation of T_H17 cells. Our findings further suggest that this mechanism commonly operates during the differentiation of both 'naturally occurring' and 'pathogenic' T_H17 cells, although additional factors certainly contribute differentially to each case[10]. The physiological nature and role of these T_H17 cells will be an interesting issue to be addressed in the context of the maintenance of intestinal mucosal homeostasis[10,12]. The actual involvement of P2 receptors and subsequent intracellular signalling mechanisms responsible for the generation of the local cytokine milieu inducing T_H17 cells are also interesting issues for future studies. Finally, elucidating the entire picture of the development of intestinal regulatory T cells, T_H17 cells and other types of cells by ATP and its metabolites (ADP and adenosine) will provide valuable information towards our understanding of the complex system of intestinal mucosal immunity as well as the establishment of innovative ATP-targeted approaches for treating patients with inflammatory bowel diseases.

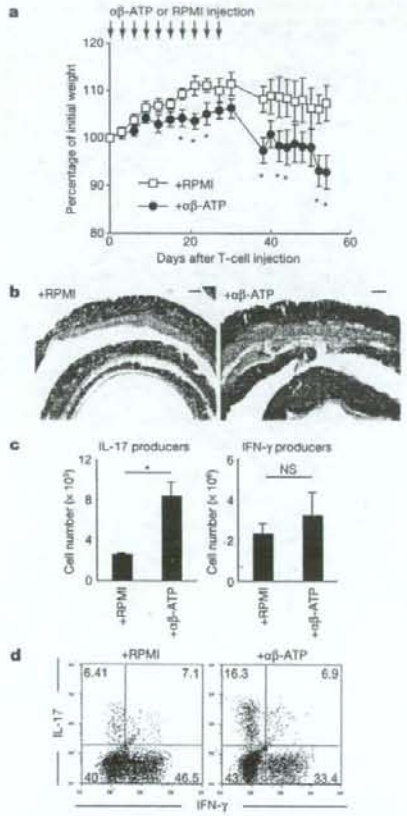

Figure 4 | Treatment with ATP exacerbates experimental colitis induced by adoptive transfer of naive $CD4^+$ T cells. SCID mice were transferred with naive $CD4^+$ T cells on day 0, and were intraperitoneally injected with αβ-ATP (1.5 mg per mouse) or RPMI 1640 medium every 3 days for 1 month. **a**, The mean body weights of SCID mice injected with αβ-ATP or RPMI ($n = 6$ per group) were monitored. Error bars, s.e.m. $^*P < 0.05$ versus RPMI-injected mice. **b**, Haematoxylin- and eosin-stained colon sections of SCID mice treated with αβ-ATP or RPMI. The numbers of IL-17- and IFN-γ-producing colonic lamina propria $CD4^+$ cells ($n = 3$ per group) are shown in **c**, and representative flow cytometry plots of $CD4^+$ T cells are shown in **d**. Error bars, s.d. $^*P < 0.02$. NS, not significant. Two independent experiments were performed with similar results.

METHODS SUMMARY

Mice, cell isolation and faecal ATP measurements. C57BL/6J mice, CB-17 SCID mice and ICR germ-free mice were purchased from CLEA Japan. Balb/c germ-free mice were maintained at the Yakult Central Institute. *Myd88*$^{-/-}$, *Trif*$^{-/-}$ and *Stat3*$^{F/F}$ Lck-Cre mice backcrossed eight or more generations onto C57BL/6J were used. The details of the procedures for isolation of lamina propria lymphocytes and $CD11c^+$ cells are described in Methods. Faeces from individual mice were weighed and suspended in PBS. The levels of ATP in the supernatants were determined with a luciferin-luciferase assay using an ATP assay kit (TOYO Ink.).

Intracellular cytokine staining and *in vitro* T-cell differentiation. The details of the procedures for intracellular cytokine staining and *in vitro* differentiation of $CD4^+$ T cells are described in Methods.

rRT–PCR. The details of the procedures and primers used for rRT–PCR are described in Methods. For all panels, bars represent the ratio of gene to *Gapdh* expression as determined by the relative quantification method (ΔΔCT) (mean + s.d. of triplicate determination).

T-cell-mediated colitis model. Naive $CD4^+CD62L^{high}$ splenic T cells from Balb/c mice were intraperitoneally transferred into SCID mice (3×10^5 cells per mouse). The mice were then injected with αβ-ATP (1.5 mg per mouse) or medium alone every 3 days for 4 weeks. After 6 or 8 weeks, colons were analysed.

Statistical analysis. Differences between control and experimental groups were evaluated using Student's *t*-test.

Full Methods and any associated references are available in the online version of the paper at www.nature.com/nature.

Received 4 June; accepted 7 July 2008.
Published online 20 August 2008.

1. Weaver, C. T., Hatton, R. D., Mangan, P. R. & Harrington, L. E. IL-17 family cytokines and the expanding diversity of effector T cell lineages. *Annu. Rev. Immunol.* 25, 821–852 (2007).
2. Bettelli, E., Oukka, M. & Kuchroo, V. K. T_H-17 cells in the circle of immunity and autoimmunity. *Nature Immunol.* 8, 345–350 (2007).
3. Ivanov, I. I. *et al.* The orphan nuclear receptor RORγt directs the differentiation program of proinflammatory IL-17$^+$ T helper cells. *Cell* 126, 1121–1133 (2006).
4. Liang, S. C. *et al.* Interleukin (IL)-22 and IL-17 are coexpressed by Th17 cells and cooperatively enhance expression of antimicrobial peptides. *J. Exp. Med.* 203, 2271–2279 (2006).
5. Nurieva, R. *et al.* Essential autocrine regulation by IL-21 in the generation of inflammatory T cells. *Nature* 448, 480–483 (2007).
6. Korn, T. *et al.* IL-21 initiates an alternative pathway to induce proinflammatory T_H17 cells. *Nature* 448, 484–487 (2007).
7. Zhou, L. *et al.* IL-6 programs T_H-17 cell differentiation by promoting sequential engagement of the IL-21 and IL-23 pathways. *Nature Immunol.* 8, 967–974 (2007).
8. Cho, J. H. & Weaver, C. T. The genetics of inflammatory bowel disease. *Gastroenterology* 133, 1327–1339 (2007).
9. Veldhoen, M., Hocking, R. J., Atkins, C. J., Locksley, R. M. & Stockinger, B. TGFβ in the context of an inflammatory cytokine milieu supports *de novo* differentiation of IL-17-producing T cells. *Immunity* 24, 179–189 (2006).
10. Mangan, P. R. *et al.* Transforming growth factor-β induces development of the T_H17 lineage. *Nature* 441, 231–234 (2006).
11. Bettelli, E. *et al.* Reciprocal developmental pathways for the generation of pathogenic effector T_H17 and regulatory T cells. *Nature* 441, 235–238 (2006).
12. Cua, D. J. & Kastelein, R. A. TGF-β, a 'double agent' in the immune pathology war. *Nature Immunol.* 7, 557–559 (2006).
13. Chang, S. Y. *et al.* Colonic patches direct the cross-talk between systemic compartments and large intestine independently of innate immunity. *J. Immunol.* 180, 1609–1618 (2008).
14. Fagarasan, S. & Honjo, T. Intestinal IgA synthesis: regulation of front-line body defences. *Nature Rev. Immunol.* 3, 63–72 (2003).
15. North, R. A. Molecular physiology of P2X receptors. *Physiol. Rev.* 82, 1013–1067 (2002).
16. Schnurr, M. *et al.* Extracellular nucleotide signaling by P2 receptors inhibits IL-12 and enhances IL-23 expression in human dendritic cells: a novel role for the cAMP pathway. *Blood* 105, 1582–1589 (2005).
17. Khakh, B. S. & North, R. A. P2X receptors as cell-surface ATP sensors in health and disease. *Nature* 442, 527–532 (2006).
18. Idzko, M. *et al.* Extracellular ATP triggers and maintains asthmatic airway inflammation by activating dendritic cells. *Nature Med.* 13, 913–919 (2007).

19. Ivanova, E. P., Alexeeva, Y. V., Pham, D. K., Wright, J. P. & Nicolau, D. V. ATP level variations in heterotrophic bacteria during attachment on hydrophilic and hydrophobic surfaces. *Int. Microbiol.* **9**, 37–46 (2006).
20. Rescigno, M. *et al.* Dendritic cells express tight junction proteins and penetrate gut epithelial monolayers to sample bacteria. *Nature Immunol.* **2**, 361–367 (2001).
21. Niess, J. H. *et al.* CX3CR1-mediated dendritic cell access to the intestinal lumen and bacterial clearance. *Science* **307**, 254–258 (2005).
22. Travis, M. A. *et al.* Loss of integrin alpha(v)beta8 on dendritic cells causes autoimmunity and colitis in mice. *Nature* **449**, 361–365 (2007).
23. Takeda, K. *et al.* Stat3 activation is responsible for IL-6-dependent T cell proliferation through preventing apoptosis: generation and characterization of T cell-specific Stat3-deficient mice. *J. Immunol.* **161**, 4652–4660 (1998).
24. Iwasaki, A. Mucosal dendritic cells. *Annu. Rev. Immunol.* **25**, 381–418 (2007).
25. Coombes, J. L. *et al.* A functionally specialized population of mucosal CD103$^+$ DCs induces Foxp3$^+$ regulatory T cells via a TGF-β and retinoic acid-dependent mechanism. *J. Exp. Med.* **204**, 1757–1764 (2007).
26. Denning, T. L., Wang, Y. C., Patel, S. R., Williams, I. R. & Pulendran, B. Lamina propria macrophages and dendritic cells differentially induce regulatory and interleukin 17-producing T cell responses. *Nature Immunol.* **8**, 1086–1094 (2007).
27. Hendriks, J. *et al.* CD27 is required for generation and long-term maintenance of T cell immunity. *Nature Immunol.* **1**, 433–440 (2000).
28. Zaba, L. C. *et al.* Amelioration of epidermal hyperplasia by TNF inhibition is associated with reduced Th17 responses. *J. Exp. Med.* **204**, 3183–3194 (2007).
29. Leach, M. W., Bean, A. G., Mauze, S., Coffman, R. L. & Powrie, F. Inflammatory bowel disease in C.B-17 scid mice reconstituted with the CD45RB^{high} subset of CD4$^+$ T cells. *Am. J. Pathol.* **148**, 1503–1515 (1996).
30. Mazmanian, S. K., Round, J. L. & Kasper, D. L. A microbial symbiosis factor prevents intestinal inflammatory disease. *Nature* **453**, 620–625 (2008).

Supplementary Information is linked to the online version of the paper at www.nature.com/nature.

Acknowledgements We thank A. Iwasaki and N. Tsuji for discussion, M. H. Jang, H. Ohno, H. Yamane, M. Yoshida and H. Shiomi for technical advice and reagents, and J. Borst for CD27-deficient mice. This work was supported by Grants-in-Aid from the Ministry of Education, Culture, Sports, Science and Technology, the Ministry of Health, Labour and Welfare, the Osaka Foundation for the Promotion of Clinical Immunology, the Ichiro Kanehara Foundation, Sumitomo Foundation, Senri Life Science Foundation and the Naito Foundation.

Author Contributions K.H. conceived the research, planned experiments and analyses and wrote the paper; K.A. and J.N. largely conducted experiments; T.S. performed some of the experiments; Y.U., M.Y., M.O., H.Y., N.I. and R.E. provided key materials; and K.T. oversaw the whole project.

Author Information Reprints and permissions information is available at www.nature.com/reprints. Correspondence and requests for materials should be addressed to K.H. (honda@ongene.med.osaka-u.ac.jp) or K.T. (ktakeda@ongene.med.osaka-u.ac.jp).

METHODS

Reagents. ATPγS (A1388), αβ-ATP (M6517) and Bz-ATP (B6396) were purchased from Sigma-Aldrich, and dissolved in phenol-red-free RPMI1640 medium. Apyrase from potato (ATPase activity: 40–200 units (U) per mg protein, A7646), suramine (S2671), TNP-ATP (T4193) and BBG (B0770) were purchased from Sigma-Aldrich, and dissolved in PBS. For *in vivo* experiments, 80 U apyrase or 250 μg of TNP-ATP was dissolved in 300 μl PBS and immediately injected intraperitoneally into SPF mice every 3 days for 15 days; or 1.25 mg of ATPγS was dissolved in phenol-red-free RPMI1640 medium and injected daily intraperitoneally or intrarectally with syringes or 1,000-μl pipette tips, respectively, into germ-free mice for 6 days. For *in vitro* experiments, ATPγS, αβ-ATP and Bz-ATP were used at 5–10 μM; suramin at 30 μM; TNP-ATP at 10 μM; BBG at 100 nM; and apyrase at 15 U ml^{-1}. The anti-IL-6 and anti-TGF-β antibodies were purchased from R&D Systems and used at 10 μg ml^{-1} or 25 μg ml^{-1}, respectively.

Mice. CB-17 SCID mice and ICR germ-free mice were purchased from CLEA Japan. Balb/c germ-free mice were maintained at the Yakult Central Institute. *Myd88*$^{-/-}$, *Trif*$^{-/-}$ and *Stat3*^{WT} Lck-Cre mice were generated as described previously[23,24], and backcrossed eight or more generations onto C57BL/6J. CD27-deficient mice were used with permission from J. Borst[25]. Unless otherwise indicated, wild-type C57BL/6J mice purchased from CLEA Japan maintained under SPF conditions were used. All experiments were performed in accordance with the Guidelines for Animal Experiments of Osaka University.

Faecal ATP measurements. Faeces from individual mice were collected, weighed and gently suspended in PBS containing 0.01% NaN_3. After centrifugation, the supernatants were collected and passed through 0.22-μm filters. The levels of ATP were determined with a luciferin-luciferase assay using an ATP assay kit (TOYO Ink) according to the manufacturer's instructions, except that the cell lysis step was omitted.

Bacterial culture. Faeces were collected from SPF mice, gently dissolved in 10 ml of serum-free RPMI medium, passed through a mesh and incubated under aerobic condition at 37 °C for 16 h. A small aliquot of the faecal suspension was transferred into 3 ml fresh medium and further incubated under aerobic conditions at 37 °C. The growth phases of these culturable intestinal aerobic commensal bacteria were monitored spectrophotometrically at 590 nm, and ATP concentrations in supernatants were measured as above. *S. typhimurium* (obtained from the Research Institute for Microbial Diseases bacterial culture collection, Osaka, Japan) was grown in the same medium, and ATP concentration was measured in the same way. The culture supernatants collected at the late exponential phase of bacterial growth were passed through 0.22-μm filters and used as conditioned media for co-culture of CD11c$^+$ cells and naive CD4$^+$ T cells.

Isolation of lymphocytes. To prepare single-cell suspensions from spleens, mesenteric lymph nodes and Peyer's patches, the collected organs were ground between glass slides, and the cells were passed through 40-μm nylon meshes and suspended in HBSS. Splenocytes were treated with RBC lysis buffer (0.15 M NH_4Cl, 1 mM $KHCO_3$, 0.1 mM EDTA) for 5 min before suspension. Naive CD4$^+$ T cells were purified from spleens using a CD4$^+$CD62L$^+$ T cell isolation kit II (Miltenyi Biotec; purity 95%). For isolation of lamina propria lymphocytes (see also ref. 3), intestines were opened longitudinally, washed to remove faecal content, and shaken in HBSS containing 5 mM EDTA for 20 min at 37 °C. After removal of epithelial cells and fat tissue, the intestines were cut into small pieces and incubated with RPMI1640 containing 4% fetal bovine serum (FBS), 1 mg ml^{-1} collagenase type II (Invitrogen), 1 mg ml^{-1} dispase (Invitrogen) and 40 μg ml^{-1} DNase I (Roche Diagnostics) for 1 h at 37 °C in a shaking water bath. The digested tissues were washed with HBSS containing 5 mM EDTA, resuspended in 5 ml of 40% Percoll (GE Healthcare) and overlaid on 2.5 ml of 80% Percoll in a 15-ml Falcon tube. Percoll gradient separation was performed by centrifugation at 780*g* for 20 min at 25 °C. The lamina propria lymphocytes were collected at the interface of the Percoll gradient and washed with MACS buffer (0.5% BSA and 2 mM EDTA in PBS) or RPMI1640. The cells were used immediately for experiments.

Isolation of lamina propria CD11c$^+$ cells. Lamina propria CD11c$^+$ cells were isolated using a protocol modified from an EDTA perfusion method[26]. Mice were anesthetized and their peritoneal and pleural cavities opened. Next, 10 ml of 20 mM EDTA in HBSS was perfused through the left ventricle of the heart. At the end of the perfusion, the entire colon or small intestine excluding the caecum was removed, opened longitudinally and washed to remove faecal content. Colons were then cut into halves and placed in tubes filled with 2 mM EDTA in HBSS. The tubes were shaken at 4,800 oscillations per min for 50 s using a mini beater (Biospec Products). The tissues were washed with PBS and the epithelial cells and muscle layers removed with tweezers. In some experiments, the epithelial cell sheets were collected and kept in ice-cold HBSS until RNA extraction. After removal of epithelial cells and muscle layers, the tissues were then cut into small pieces and incubated with RPMI1640 containing 4% FBS, 1 mg ml^{-1} collagenase type II, 1 mg ml^{-1} dispase and 40 μg ml^{-1} DNase I for 1 h at 37 °C in a shaking water bath. After filtration of the digested tissues through a 40-μm cell strainer, the isolated cells were washed with MACS buffer and CD11c-positive cells were purified twice to >95% purity using CD11c MicroBeads (Miltenyi Biotec). In some experiments, enriched CD11c-positive cells were further stained with specific antibodies and sorted by FACSVantageSE (BD Biosciences), with a resulting purity of around 95%.

Isolation of splenic CD11c$^+$ cells. Spleens were collected and incubated with RPMI1640 containing 4% FBS, 1 mg ml^{-1} collagenase type II, 1 mg ml^{-1} dispase and 40 μg ml^{-1} DNase I for 1 h at 37 °C in a shaking water bath. After treatment with RBC lysis buffer, the isolated cells were washed with MACS buffer and CD11c-positive cells purified twice to >95% purity using CD11c MicroBeads (Miltenyi Biotec).

Intracellular cytokine staining. The intracellular expression of IL-17 and IFN-γ in CD4$^+$ T cells was analysed using a Cytofix/Cytoperm Kit Plus (with Golgistop; BD Biosciences) according to the manufacturer's instructions. In brief, lymphocytes obtained from the intestinal lamina propria, spleens, mesenteric lymph nodes or Peyer's patches were incubated with 50 ng ml^{-1} phorbol myristate acetate (PMA; Sigma), 5 μM calcium ionophore A23187 (Sigma) and Golgistop in complete media at 37 °C for 4 h. Surface staining was performed with a corresponding cocktail of fluorescently labelled antibodies for 20 min at 4 °C; after this, the cells were permeabilized with Cytofix/Cytoperm solution for 20 min at 4 °C and intracellular cytokine staining was performed with fluorescently labelled cytokine antibodies for 20 min.

***In vitro* T-cell differentiation.** Naive CD4$^+$ T cells were collected for 4 days with purified CD11c$^+$ cells and 0.5 μg ml^{-1} anti-CD3 antibody (BD Biosciences) in the presence or absence of ATP. The cultured cells were harvested and rested for 2 h before being restimulated with PMA and calcium ionophore (Sigma) for 3 h.

Flow cytometry. The following antibodies were used: anti-CD4-Cychrom, anti-IFN-γ-FITC, anti-IL-17-PE, anti-CD8-FITC, anti-CD11b-PE, anti-CD11b-FITC, anti-CD11c-PE, anti-CD11c-APC, anti-CD80-FITC, anti-CD103-FITC (all BD Biosciences), anti-CCR6-PE (R&D Systems Inc.), anti-F4/80-Alexa488 (Caltag Laboratories), anti-CD70-biotin (eBioscience), rabbit anti-CX3CR1 antibody (Torrey Pines Biolabs), streptavidin-Alexa488 and goat anti-rabbit IgG-Alexa488 (Molecular Probes). Data were acquired using a FACSCalibur or a FACSCanto (BD Biosciences) and analysed using Flowjo software (Tree Star).

Real-time RT–PCR. Complementary DNAs were synthesized from RNA samples prepared with an RNeasy Mini Kit (Qiagen) using Rever Tra Ace (Toyobo). Complementary DNAs were analysed by rRT–PCR using Power SYBR Green PCR Master Mix (Applied Biosystems) in an ABI 7300 real time PCR system (Applied Biosystems). Serial dilutions of a standard were included for each gene to generate a standard curve and allow calculation of the input amount of cDNA for each gene. Values were then normalized by the amount of GAPDH in each sample. The primer sets were designed with Primer Express Version 3.0 (Applied Biosystems) and initially tested to confirm comparable (>90%) efficiencies. The following primer sets were used: *Il17a*, 5′-GGACTCTCCACCGCAATGA-3′ and 5′-GGCACTGAGCTTCCCAGATC-3′; *Il17f*, 5′-CCCCATGGGATTACAACATCAC-3′ and 5′-CATTGATGCAGCCTGAGTGTCT-3′; *Il21*, 5′-GGCAATGAAAGCCTGTGGAA-3′ and 5′-GGCAATGAAAGCCTGTGGAA-3′; *Rorc*, 5′-GGAGGACAGGGAGCCAAGTT-3′ and 5′-CCGTAGTGGATCCCAGATGACT-3′; *Ifng*, 5′-TCAAGTGGCATAGATGTGGAAGAA-3′ and 5′-TGGCTCTGCAGGATTTTCATG-3′; *Il4*, 5′-GGCATTTTGAACGAGGTCACA-3′ and 5′-GACGTTTGGCACATCCATCTC-3′; *Il6*, 5′-CTGCAAGAGACTTCCATCCAGTT-3′ and 5′-AAGTAGGGAAGGCCGTGGTT-3′; *Itgb8*, 5′-ACAGCATCGCATGGACCAA-3′ and 5′-AAGCAACCCGATCAAGAATGTG-3′; *Itgav*, 5′-CGCCTATCTTCGGGATGAATC-3′ and 5′-CCAACCGATACTCCATGAAAATG-3′; *Gapdh*, 5′-CCTCGTCCCGTAGACAAAATG-3′ and 5′-TCTCCACTTTGCCACTGCAA-3′; *P2rx1*, 5′-ACGAAACAAGAAGGTGGGAGT-3′ and 5′-AGGCCACTTGAGGTCTGGTAT-3′; *P2rx2*, 5′-GAGAGCTCCATCATCACCAAA-3′ and 5′-CAGGGTCTGGGAAGGAGTAAC-3′; *P2rx3*, 5′-CCGAGAACTTCACCATTTTCA-3′ and 5′-TTTATGTCCTTGTCGGTGAGG-3′; *P2rx4*, 5′-TGGCTACAATTTCAGGTTTGC-3′ and 5′-GATCATGGTTGGGATGATGTC-3′; *P2rx5*, 5′-AACCGTCTGGACAACAAACAC-3′ and 5′-TTTCATCAGGTCACGGAACTC-3′; *P2rx7*, 5′-CCAGGAAGCAGGAGAGAACTT-3′ and 5′-ATCCGTGTTCTTGTCATCCAG-3′; *P2ry1*, 5′-GGCAGGCTCAAGAAGAAGAAT-3′ and 5′-TCCCAGTGCCAGAGTAGAAGA-3′; *P2ry2*, 5′-CCGAGAGCTCTTTAGCCATTT-3′ and 5′-GCCATAAGCACGTAACAGACC-3′; *P2ry6*, 5′-CTCACCTGCATTAGCTTCCAG-3′ and 5′-ACACGACTCCACACACTACCC-3′; *P2ry12*, 5′-GTTCCTGGGGTTGATAACCAT-3′ and 5′-GCCCAGATGACAACAGAAAGA-3′; *P2ry13*, 5′-CGTTCAGGAAAACCTTTGTCA-3′ and 5′-

ACACTTCTTCACGGATGATGG-3′. The *Tnf*, *Il22* and *Il23a* primer and probe (FAM MGB Probe) were purchased from Applied Biosystems.

ELISA for faecal IgA. Faeces (50–100 mg) were collected from individual mice, weighed and homogenized in 100 μl of PBS containing 0.01% NaN_3 per 10 mg of faeces. After centrifugation at 9,000*g* for 5 min, the supernatants were collected and diluted by 1:1,000. IgA levels were determined by ELISA using a mouse IgA ELISA quantitation kit (Bethyl Laboratories) and TMB solution (eBioscience). Optical densities were determined at a wavelength of 450 nm with a reference wavelength of 570 nm.

T-cell-mediated colitis model. Naive $CD4^+CD62L^{high}$ splenic T cells from Balb/c mice were purified and intraperitoneally transferred into SCID mice (3×10^5 cells per mouse). The mice were then injected with αβ-ATP in RPMI (1.5 mg per mouse) or medium alone every 3 days for 4 weeks. After 8 weeks, the colons were examined for the numbers of IL-17- and IFN-γ-producing $CD4^+$ cells or analysed histologically after haematoxylin and eosin staining.

31. Yamamoto, M. *et al.* Role of adaptor TRIF in the MyD88-independent Toll-like receptor signaling pathway. *Science* **301**, 640–643 (2003).
32. Mizoguchi, E. *et al.* Colonic epithelial functional phenotype varies with type and phase of experimental colitis. *Gastroenterology* **125**, 148–161 (2003).

Am J Physiol Gastrointest Liver Physiol 296: G23–G35, 2009.
First published November 20, 2008; doi:10.1152/ajpgi.90225.2008.

Requirement of Notch activation during regeneration of the intestinal epithelia

Ryuichi Okamoto,[1,2] Kiichiro Tsuchiya,[2] Yasuhiro Nemoto,[2] Junko Akiyama,[2] Tetsuya Nakamura,[1,2] Takanori Kanai,[2] and Mamoru Watanabe[2]

[1]*Department of Advanced Therapeutics in Gastrointestinal Diseases and* [2]*Department of Gastroenterology and Hepatology, Graduate School, Tokyo Medical and Dental University, Tokyo, Japan*

Submitted 7 March 2008; accepted in final form 18 November 2008

Okamoto R, Tsuchiya K, Nemoto Y, Akiyama J, Nakamura T, Kanai T, Watanabe M. Requirement of Notch activation during regeneration of the intestinal epithelia. *Am J Physiol Gastrointest Liver Physiol* 296: G23–G35, 2009. First published November 20, 2008; doi:10.1152/ajpgi.90225.2008.—Notch signaling regulates cell differentiation and proliferation, contributing to the maintenance of diverse tissues including the intestinal epithelia. However, its role in tissue regeneration is less understood. Here, we show that Notch signaling is activated in a greater number of intestinal epithelial cells in the inflamed mucosa of colitis. Inhibition of Notch activation in vivo using a γ-secretase inhibitor resulted in a severe exacerbation of the colitis attributable to the loss of the regenerative response within the epithelial layer. Activation of Notch supported epithelial regeneration by suppressing goblet cell differentiation, but it also promoted cell proliferation, as shown in in vivo and in vitro studies. By utilizing tetracycline-dependent gene expression and microarray analysis, we identified a novel group of genes that are regulated downstream of Notch1 within intestinal epithelial cells, including PLA2G2A, an antimicrobial peptide secreted by Paneth cells. Finally, we show that these functions of activated Notch1 are present in the mucosa of ulcerative colitis, mediating cell proliferation, goblet cell depletion, and ectopic expression of PLA2G2A, thereby contributing to the regeneration of the damaged epithelia. This study showed the critical involvement of Notch signaling during intestinal tissue regeneration, regulating differentiation, proliferation, and antimicrobial response of the epithelial cells. Thus Notch signaling is a key intracellular molecular pathway for the proper reconstruction of the intestinal epithelia.

intestinal epithelial cells; goblet cells; PLA2G2A; ulcerative colitis

THE INTESTINAL EPITHELIA are composed of four lineages of intestinal epithelial cells (IECs) that arise from intestinal stem cells (1). Recent studies have shown that various signals such as Wnt, Sonic hedgehog, and bone morphogenetic protein interact within the stem and progenitor cells of the intestinal epithelia to finely regulate the expansion and the cell fate decision of IECs. Other studies have revealed that Notch signaling may also play critical roles in the maintenance of the intestinal epithelia (20).

Notch signaling is a signaling pathway known to regulate differentiation and proliferation of cells in diverse adult tissues (1). Activation of Notch receptor is mediated by the cleavage of its intracellular domain (NICD), and this intracellular domain translocates from the cell membrane to the nucleus, thereby functioning as a transcriptional activator of target genes such as Hes1 (10, 25). The functional role of Notch signaling in the intestine was first described in a study of Hes1-null mice; depletion of Hes1 was associated with significant increases in the secretory lineage IECs (9). Other studies have shown that the activation of Notch promoted proliferation of crypt progenitor cells and directed their cell fates toward absorptive but not secretory lineage cells (6, 28, 33). A recent study suggested that Notch might also function in postmitotic IECs, directing their cell fates toward secretory lineage cells (42). Thus these studies have suggested that Notch signaling functions in the intestine to regulate differentiation and proliferation of IECs, contributing to the maintenance and the homeostasis of the intestinal mucosa. However, the role of Notch signaling in tissue regeneration is less understood.

Damage of the intestinal epithelia is observed in a wide variety of diseases, such as acute intestinal infections, radiation injuries, or idiopathic inflammatory bowel diseases (23). Once the epithelial layer is damaged, it responds by restoring the continuity and integrated structure via activating the stepwise regeneration program (16). The initial response is called restitution, which is the redistribution of remaining IECs to rapidly cover the damaged area. This initial step is usually completed in an extremely short period of time and thus does not require the proliferation or expansion of IECs (19). However, in the next step, the rapid expansion of IECs is necessary to rebuild the proper structure of the epithelia. This response is manifested by the appearance of the regenerative epithelia in the intestine, showing a marked expansion of the proliferating compartment consisting of undifferentiated IECs. However, the exact molecular mechanisms involved in this critical step of intestinal epithelial regeneration has never been described.

Another change that is observed in the intestine during such a regenerative process is the ectopic expression of antimicrobial peptides by IECs. Paneth cells usually secrete peptides such as lysozymes, α-defensins, or PLA2G2A, and this helps to maintain the ideal environment for the stem and progenitor IECs within the small intestinal crypts. The ectopic expressions of these antimicrobial peptides by IECs are frequently observed in the inflamed colonic mucosa (5, 8), and such expressions likely support the local immune system in providing an ideal environment for the regeneration of the damaged mucosa.

In this study, we show that Notch signaling is activated in many IECs in the inflamed mucosa of murine colitis. Results show that the activation of Notch is critical for the proper regeneration program in the epithelial layer and that it helps to suppress goblet cell differentiation and promote cell proliferation. A comprehensive analysis identified a novel group of genes regulated by Notch in IECs, which included

Address for reprint requests and other correspondence: M. Watanabe, Dept. of Gastroenterology and Hepatology, Graduate School, Tokyo Medical and Dental Univ., 1-5-45 Yushima, Bunkyo-ku, Tokyo 113-8519, Japan (e-mail address: mamoru.gast@tmd.ac.jp).

The costs of publication of this article were defrayed in part by the payment of page charges. The article must therefore be hereby marked "*advertisement*" in accordance with 18 U.S.C. Section 1734 solely to indicate this fact.

a gene encoding an antimicrobial peptide called PLA2G2A. Such functions of Notch activation were present not only in the mice intestine but also in the human intestine. Finally, the clinical relevance of Notch-mediated regeneration is analyzed in ulcerative colitis (UC). Thus Notch signaling is a key-signaling pathway involved in intestinal tissue regeneration, in fine regulation of differentiation and proliferation, and in antimicrobial activities in IECs. Our findings point to a novel molecular target for agents that could promptly regenerate the intestinal mucosa in a wide range of intestinal diseases.

MATERIALS AND METHODS

Mice. C57BL/6J mice at 8 wk of age were purchased from Japan Clea. Mice were housed and maintained in the animal facility of Tokyo Medical and Dental University. The institutional animal use and care committee approved the study.

In vivo experiments. Induction of colitis was performed as previously described (17). Briefly, mice were fed ad libitum with 1.75% dextran sodium sulfate (DSS, Bio Research of Yokohama) for 5 consecutive days, followed by distilled water for another 5 days. For inhibition of Notch activation, mice were orally administered with either 5% DMSO (vehicle, VEC) or LY411,575 (LY) (10 mg/kg) dissolved in 0.5% (wt/vol) methylcellulose (WAKO), once daily for 5 consecutive days. Twenty-four mice were separated into four groups: *1*) fed distilled water for five days followed by daily administration of vehicle alone (VEC, $n = 6$) for 5 days, *2*) fed distilled water for 5 days followed by daily administration of LY411,575 (LY, $n = 6$) for five days, *3*) fed 1.75% DSS for 5 days followed by daily administration of vehicle (DSS + VEC, $n = 6$) for 5 days, and *4*) fed 1.75% DSS for 5 days followed by daily administration of LY411,575 (DSS + LY, $n = 6$) for 5 days. The whole body weights of mice were measured everyday. They were euthanized 12 h after the final administration. Colonic tissues were subjected to hematoxylin and eosin staining and analyzed by histological scoring following the criteria described elsewhere (21). Flow cytometry of thymocytes and splenocytes were performed as previously described (35, 41).

Immunoblot analysis. Immunoblots were performed as described elsewhere (18). The primary antibodies used were anti-Cleaved Notch1 (1:1,000, Cell Signaling Technology), anti-Hes1 (1:4,000, a kind gift from Dr. T. Sudo), and anti-β-actin (1:5,000, Sigma). Proteins were visualized either by the ECL Advance Western Blotting Kit (GE Healthcare) or ECL Western Blotting Kit (GE Healthcare).

Cell culture. The cell cultures and transfections of plasmid DNA were performed as described elsewhere (18). The inhibition of Notch signaling was achieved by the addition of LY411,575 (1 μM), synthesized according to Wu et al. (38). A cell line expressing Notch1 intracellular domain (Tet-On NICD1 cells) under the control of tetracycline or doxycycline (DOX, 100 ng/ml, Clontech) was generated as described elsewhere (18), using LS174T cells as parent cells. The cell lines were supplemented with Blastcidin (7.5 μg/ml, Invitrogen) and Zeocin (750 μg/ml, Invitrogen) for their maintenance.

RT-PCR assays. RT-PCR was performed as described elsewhere (18). Quantitative analyses using the SYBR green master mix (Qiagen) was performed by ABI 7500 (Applied Biosystems). Primer sequences for human β-actin, G3PDH, or MUC2 have been previously described (30). The primer sequences for other genes are summarized in Table 1. The results are shown as the means of the data collected from two rounds of assays, with each assay performed in triplicate. The data were statistically analyzed with paired Student's *t*-tests.

Human intestinal tissue specimens. Human tissue specimens were obtained from patients who underwent surgery for the treatment of Crohn's disease, UC, or colon cancer at Yokohama Municipal General Hospital or Tokyo Medical and Dental University Hospital. Written informed consent was obtained from each patient, and the study was approved by the ethics committee of Yokohama Municipal General Hospital and Tokyo Medical and Dental University.

Immunohistochemistry. Immunohistochemistry using intestinal tissues has been described elsewhere (12). The same antibodies used in immunoblot analysis were also used for the immunohistological staining of NICD1 and Hes1. The other antibodies used were anti-human Ki-67 (1:50, MIB-1, DAKO), anti-human PLA2G2A (1:200, sc-14468, Santa Cruz Biotechnology), anti-human MUC2 (1:100, Ccp58, Santa Cruz Biotechnology), and anti-mouse Ki-67 (1:50, TEC-3, DAKO). Microwave treatment (500 W, 10 min) in 10 mM citrate buffer was required for staining human tissues in Hes1, Ki-67, and NICD1 and for staining mice tissues in Ki-67. The tyramide signal amplification (Molecular Probes) was used for immunofluorescent detection of NICD1. Staining was visualized by an avidin-biotin-peroxidase complex (ABC) elite kit (Vector) using diaminobenzidine as a substrate or by secondary antibodies conjugated with Alexa-594 or Alexa-488 (Molecular Probes). The quantification of Hes1 (Fig. 1*B*), Alcian blue, Ki-67, or NICD1 (Fig. 8*B*) was conducted by the examination of nine randomly selected longitudinal sections of crypts selected from at least three different individuals. The data were statistically analyzed with paired Student's *t*-tests.

Microarray. Microarray analysis was performed using the Acegene human oligo chip 30K subset A (Hitachi software). Total RNA was collected before and after 24 h of NICD1 expression in LS174T cells and labeled using the Amino Aryll Message Amp aRNA kit (Ambion). The complete dataset of the analysis has been submitted to the NCBI Gene Expression Omnibus (GEO) and is accessible through GEO accession number GSE10136.

Table 1. *Primers used in the present study*

Gene	Primer Sequence	
	Forward	Reverse
Human Hes1	5′- ATGCCAGCTGATATAATGGAG -3′	5′- TCACCTCGTTCATGCACTCG -3′
Human Notch1	5′- CCGAACCAATACAACCCTCT -3′	5′- GCGATCTGGGACTGCTGCATGCT -3′
Human PLA2G2A	5′- ACCATGAAGACCCTCCTACTG -3′	5′- GAAGAGGGGACTCAGCAACG -3′
Mouse Hes1	5′- TCAACACGACACCGGACAAACC -3′	5′- GGTACTTCCCCAACACGCTCG -3′
Mouse MUC2	5′- TCCACGATGGGGCTGCCACT -3′	5′- GGCCCGAGAGTAGACCTTGG -3′
Mouse TNF-α	5′- CTACTGGCGCTGCCAAGGCTGT -3′	5′- GCCATGAGGTCCACCACCCTG -3′
Mouse IFN-γ	5′- ACACTGCATCTTGGCTTTGC -3′	5′- CGGATGAGCTCATTGAATGCT -3′
MouseIL-1α	5′- CCCGTCGTTAAAGCTGTCTG -3′	5′- AATTGGAATCCAGGGGAAAC -3′
Mouse IL-1β	5′- TTGACGGACCCCAAAAGAT -3′	5′- GAAGCTGGATGCTCTCATCTG -3′
Mouse IL-6	5′- GCTACCAAACTGGATATAATCAGGA -3′	5′- CCAGGTAGCTATGGTACTCCAGAA -3′
Mouse PLA2G2A	5′- AAGAAGCCCAAATGCTGAAA -3′	5′- TTTATCACCGGGAAACTTGG -3′
Mouse β-actin	5′- CCTAAGGCCAACCGTGAAAAG -3′	5′- TCTTCATGGTGCTAGGAGCCA -3′

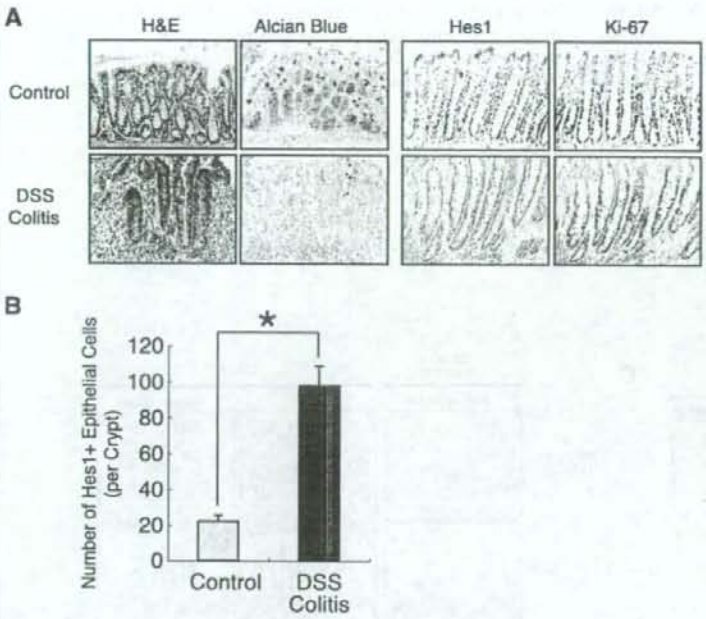

Fig. 1. Activation of Notch signaling is increased in crypts of dextran sodium sulfate (DSS)-induced colitis. *A*: histological analysis of DSS-induced colitis showing a decrease in mucin-producing intestinal epithelial cells (IECs) and an increase in Hes1- and Ki-67-expressing IECs within the crypts of the colitic mucosa. Blue staining with Alcian blue represents mucin production, whereas brown staining with diaminobenzidine (DAB) shows positive staining for Hes1 or Ki-67 (original magnification ×400). *B*: quantitative analysis of Hes1-positive IECs in crypts of normal or colitic mucosa. Data are shown as number of Hes1-positive cells per crypt on the basis of the analysis of immunohistochemical stainings. Error bars represent SD. $*P < 0.05$ on the Student's *t*-test. H & E, hematoxylin and eosin.

Plasmids. Hes1p-Luc, containing six tandem-repeats of the RBP-Jk binding site, was a kind gift from Dr. Kageyama (Kyoto, Japan). PLA2-Luc was generated by cloning a 2778-bp sequence 5′ of the human PLA2G2A gene (corresponding to −2,758 to + 20 of the promoter region) into a pGL3 basic vector (Promega). MUC2-Luc (40) was a kind gift from Dr. Yuasa (Tokyo, Japan). Tetracycline-dependent expression of NICD1 was achieved by cloning the gene encoding the intracellular portion of the mouse Notch1 (amino acid 1,704-2,531) into the pcDNA4/TO/myc-his vector (Invitrogen). All constructs were confirmed by DNA sequencing.

Immunostaining of cultured cells. Staining of cultured cells has been previously described (30). Detection of the MUC2 antibody was carried out either by the standard ABC method or by the Alexa 594-conjugated secondary antibody (Molecular Probes). The quantification of cells positive for MUC2 staining was performed by examining six randomly selected fields (three fields each in two individual counts) under ×400 magnification. The data were statistically analyzed with paired Student's *t*-tests.

ELISA. For PLA2G2A protein quantification, 1×10^6 cells were cultured in 2 ml of medium with or without DOX and analyzed with the human-PLA2 enzyme immunoassay kit (Cayman Chemicals). The incorporation of BrdU was examined by seeding cells at various cell densities in the 96-well plate, supplemented with DMSO or LY411,575. The BrdU was added 8 h before the end of culture, and the cells were subjected to analysis with the cell proliferation ELISA kit (Roche Diagnostics). The results are shown as the means of data collected by two rounds of assays, with each assay performed in triplicate. The data were statistically analyzed with paired Student's *t*-tests.

Reporter assays. The reporter assay was performed as previously described (18). Each assay was performed in triplicate, and the results were normalized using the *Renilla* luciferase activity. The results are shown as the means of normalized arbitrary units, and the data were statistically analyzed with paired Student's *t*-tests.

RESULTS

Hes1 is expressed in crypt epithelial cells of DSS-colitis. Since previous studies have evaluated the contribution of Notch signaling in the maintenance of mice intestinal epithelium (28, 33, 34), we sought to examine the role of Notch signaling in mice colitis. At first, we analyzed the expression of Hes1, a direct target gene of Notch, in mice with colitis induced by the oral administration of DSS (DSS-colitis, Fig. 1*A*). In the normal colon, crypts are predominantly composed of mature goblet cells that produce mucin. In such crypts, Hes1 is expressed in IECs residing at the lowest part of the crypt, which is also where Ki-67-positive IECs are found. In sharp contrast, the clear loss of mucin production was observed in the inflamed mucosa of DSS-colitis mice. The expressions of both Hes1 and Ki-67 were observed in a larger population of IECs, which were distributed from the bottom to the most upper regions of the crypt, suggesting that Notch signaling was activated in these IECs. The quantitative analysis of the immunostaining revealed significant increases in Hes1-positive IECs within the crypts of the DSS-colitis mice (Fig. 1*B*). These findings suggested that Notch signaling is activated in a greater number of IECs in DSS-colitis, which might be closely related with the greater number of proliferating IECs and the loss of mucin-producing IECs.

LY411,575 inhibits Notch activation and promotes goblet cell differentiation in mice intestine. To further examine the role of Notch signaling in colitis, we used LY411,575, a γ-secretase inhibitor (GSI) that is known to block Notch activation in vivo (14, 27, 36). Oral administration of LY411,575 for 5 consecutive days significantly reduced the expression of

Hes1 mRNA in mice intestine, suggesting that Notch activation was inhibited (Fig. 2*A*). In contrast, the expression of MUC2 mRNA was significantly increased by LY411,575, suggesting that the number of goblet cells increased. Consistent with this, histological analysis showed marked increases in mucus-producing IECs in the intestines of the LY411,575-treated mice (Fig. 2*C*). Consistent with reports from previous studies (27, 36), these results showed that LY411,575 could